

# Assessment of the environmental, ecosystem, and human activities in coastal Vietnam and Cambodia gathered from satellite remote sensing

Helen S. Findlay, Andrey Kurekin, Nick Selmes

December 2022



# Assessment of the environmental, ecosystem, and human activities in coastal Vietnam and Cambodia gathered from satellite remote sensing

This project was funded by UK Research and Innovation, as part of the Natural Environment Research Council's Official Development Assistance – National Capability project Addressing Challenges of Coastal Communities through Ocean Research for Developing Economies (ACCORD) through grant NE/R000123/1.

## Authors

Helen Findlay<sup>(1)</sup>, Andrey Kurekin <sup>(1)</sup>, Nick Selmes

1) Plymouth Marine Laboratory, Prospect Place, Plymouth, UK, PL1 3DH.

## Contact

Dr Helen Findlay (hefi@pml.ac.uk)  
Plymouth Marine Laboratory  
Prospect Place  
The Hoe  
Plymouth  
Devon, UK  
PL1 3DH

## Suggested citation:

H Findlay, A Kurekin, N Selmes (2022). Assessment of the environmental, ecosystem, and human activities in coastal Vietnam and Cambodia gathered from satellite remote sensing. PML Publishing, pp 138 DOI: <https://doi.org/10.17031/p1rp-f869>

# Contents

|  |           |
|--|-----------|
| <b>Executive summary</b> .....   | <b>2</b>  |
| <b>1. Introduction</b> .....   | <b>3</b>  |
| 1.1. The ACCORD project.....   | 3         |
| 1.2. Report aims .....   | 3         |
| 1.3. Da Nang, Vietnam .....  | 4         |
| 1.4. Kep province, Cambodia .....  | 4         |
| <b>2. Methods</b> .....  | <b>5</b>  |
| 2.1. Earth observations for environmental assessment   | 5         |
| 2.1.1. Introduction .....  | 5         |
| 2.1.2. Sea Surface Temperature (SST)   | 5         |
| 2.1.3. Water quality .....   | 5         |
| 2.1.4. Chlorophyll a concentration at 1 km: Copernicus Climate Change Initiative:<br>Ocean Colour (OC-CCI) (Sathyendranath et al., 2019) | 6         |
| 2.1.4.1. Chlorophyll a concentration and turbidity processed with PML's<br>Calimnos processor.....                                       | 7         |
| 2.1.4.2. ....300 m dataset: Envisat MERIS and Sentinel 3 OLCI  | 7         |
| 2.1.4.3. ....60 m dataset: Sentinel 2 MSI  | 7         |
| 2.1.5. Data access .....   | 7         |
| 2.1.6. Statistical analysis.....   | 7         |
| 2.2. Earth Observations for mapping location of aquaculture sites  | 8         |
| 2.2.1. EO methods .....  | 8         |
| 2.2.2. Study region and datasets .....   | 10        |
| 2.2.3. Methodology and data processing chain   | 11        |
| <b>3. Results</b> .....  | <b>14</b> |
| 3.1. Vietnam environmental assessment ...  | 14        |
| 3.1.1. Large scale regional analysis (13 – 19 °N; 106 – 112 °E)  | 14        |
| 3.1.2. Da Nang local analysis (300 m & 60 m datasets)  | 16        |
| 3.2. Cambodia environmental assessment   | 19        |
| 3.2.1. Large scale regional analysis (9 – 11 °N; 103 – 105 °E)   | 19        |
| 3.2.2. Kep province local analysis (300 m resolution)  | 21        |
| 3.3. Da Nang aquaculture assessment .....  | 23        |
| <b>4. Discussion</b> .....   | <b>29</b> |
| 4.1. Earth observations for environmental assessment   | 29        |
| 4.2. Earth Observations for mapping location of aquaculture sites  | 29        |
| <b>7. References</b> .....   | <b>31</b> |

# Executive summary

Within the ACCORD (Addressing Challenges of Coastal Communities through Ocean Research for Developing Economies) project, satellite Earth Observations are used for two purposes: 1. To describe basic environmental dynamics around two focus regions, Da Nang Bay in Vietnam and Kep Province in Cambodia. Two aspects of satellite data are examined for this purpose: first, sea surface temperature (SST); second, water quality data, focussing on chlorophyll a and turbidity. 2. To assess the potential for mapping locations of aquaculture sites around Da Nang Bay, Vietnam, through exploitation of EO data. This second purpose utilises the sea surface radar backscattering coefficient.

NOAA's Pathfinder SST dataset derived from measurements made by AVHRR sensors was used here at 4 km resolution. This dataset offers a long time series, which has gone through rigorous quality control and calibration, and as such is considered a climate-quality dataset. The seasonal cycle as well as the long term dynamics for SST can be observed, showing the monsoon dynamics of the region. No trend in warming over the past two decades is observable from these data.

Water quality measurements were investigated using a number of EO-derived products. These products cover different spatial and temporal scales. The first is the ESA Ocean Colour Climate Change Initiative (OC-CCI) – Chlorophyll a dataset. This has a 1 km resolution and is mainly optimised for the open ocean through to moderately turbid coastal waters; the most turbid coastal waters around Da Nang and Kep are frequently masked in this dataset. Larger scale regional seasonality and long term changes in chlorophyll levels are assessed. There is no clear trend through time over the wider regions, however clear spatial dynamics can be observed. The relationship between chlorophyll a and SST over the past two decades was also investigated. Higher levels of chlorophyll a occurred near the coasts at certain times of year, predominantly corresponding to seasonal changes in temperature and increases in river flow during monsoon periods.

The coastal and nearshore water quality around Da Nang and Kep was assessed using datasets processed with PML's Calimnos processor, which includes a blend of algorithms designed for very turbid water and prioritises higher spatial resolution over having the longest time series. The 300 m dataset were derived from Envisat MERIS and Sentinel 3 OLCI, which provide a medium-term time series, although there is a four year gap between the missions so a continuous dataset is not available. These data offer the best balance of resolution and algorithm performance for coastal remote sensing at present. The 60 m water quality dataset was derived from Sentinel 2 MSI, which has been operating since 2015 and hence is a shorter time series. However, the 60 m dataset is especially useful for resolving smaller features, as is demonstrated by highlighting small eddy features and river outflows around both Da Nang bay and Kep.

The method for detecting and mapping aquaculture structures, such as finfish cages, shellfish farms and floating houses using freely available Sentinel-1A SAR sensor data was successfully applied to Da Nang bay and nearby rivers. 11 aquaculture sites were identified in the bay and in the rivers, confirmed by comparing with high resolution Google Map satellite images. Comparing static maps across different years shows that this method can be used to monitor temporal changes in detected aquaculture sites.

# 1. Introduction

## 1.1. The ACCORD project

The NERC-funded National Capability project “Addressing Challenges of Coastal Communities through Ocean Research for Developing Economies” (ACCORD) is a consortium project that aimed to deliver high-quality science outcomes required to improve the environmental information available to support: 1) Sustainable growth of, and resilience to change for, the blue economies of partner countries, and 2) Resilience to natural hazards including impact-based, climate-proof coastal flood warning systems, in coastal states on the Development Assistance Committee (DAC) list of Official Development Assistance (ODA) recipients. As part of ACCORD, PML has been working with two communities, one in Vietnam and one in Cambodia (Figure 1). Over the period 2018 to 2021, research and capacity building was carried out in these two locations. One aspect of these programmes was to utilise Earth Observations as a tool for providing background data.

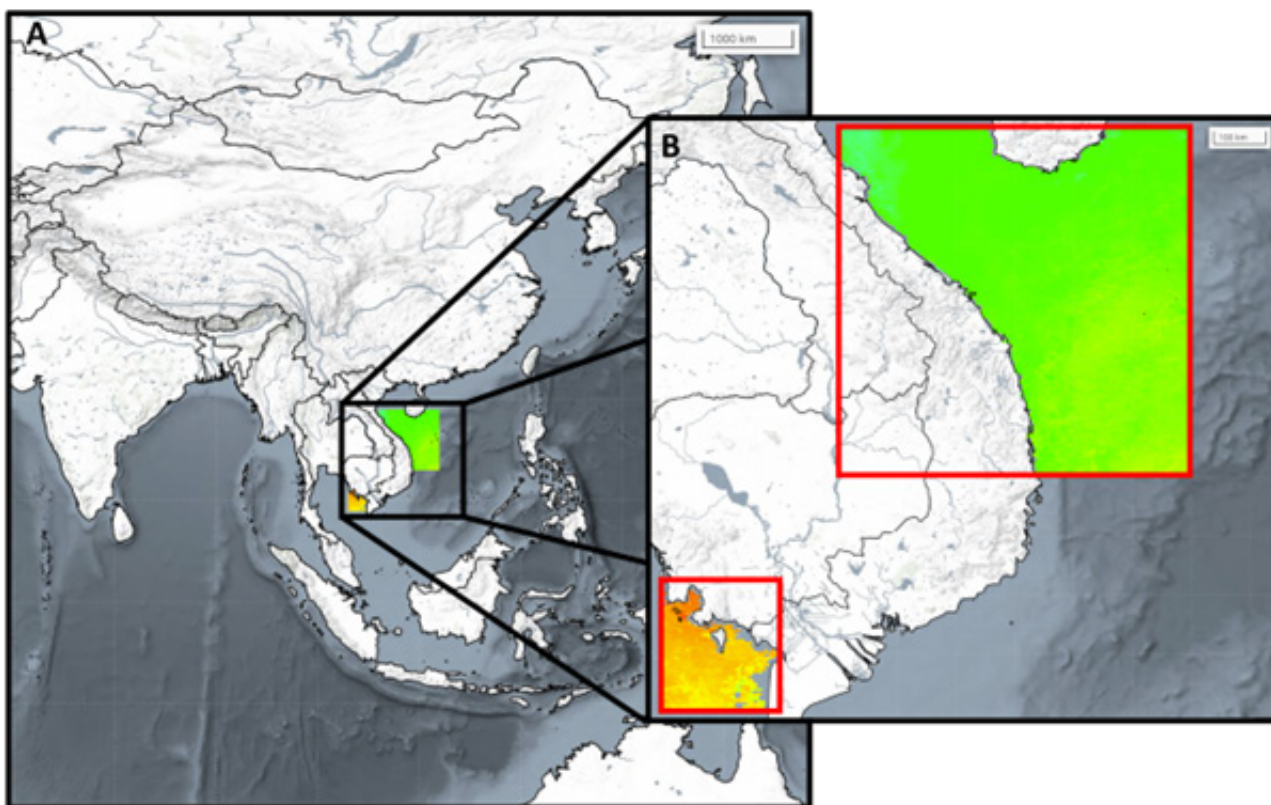


Figure 1: Maps of study locations. A) Map showing South East Asia region. B) Map showing large scale remote sensing boundaries (red boxes) around Cambodia and Vietnam.

## 1.2. Report aims

The aim of this report is to describe the Earth observation (EO) data collected for these two communities during the ACCORD project, and use the data to describe the basic environmental and ecosystem dynamics around Da Nang, Vietnam in particular, but also around the Kep Province, Cambodia. We also assess the potential for mapping locations of aquaculture sites around Da Nang Bay through exploitation of EO data. Here, we first describe the locations and background for studying these two sites before moving on to the methodology, results, and discussion.

### 1.3. Da Nang, Vietnam

The service and construction sectors, including fisheries, agriculture, and aquaculture, strongly support an aspiration to develop Da Nang's coastal economy. The coastal environment and its associated marine habitats are a key attraction for the tourism sector which seeks to realise its employment and revenue-generating potential through significant expansion. The development of coastal infrastructure, including a commercial seaport, will add to the growth of Da Nang's coastal economy. The marine environment provides valuable ecosystem services that will support this economic growth. These ecosystem services remove, store and export nutrients and carbon, which maintain high water quality, underpinning tourism, fisheries, and aquaculture while contributing to the well-being of local communities. However, the marine environment's existing capacity to provide this service is unknown. Understanding this capacity and its supporting factors through the provision of scientific evidence is crucial for ecosystem management and planning decisions. Managing this capacity in line with the growth of Da Nang's coastal economy will ensure that the marine environment and associated habitats remain resilient.

### 1.4. Kep province, Cambodia

The province of Kep has been designated as an area for nature and tourism. The marine-based activities with highest economic value are tourism and fisheries, with the blue-crab fishery being of particularly high value (Rendon et al., 2022). There is a drive to increase the level of tourism in this area, with development of tourism infrastructure along the coast. The coastal region has a variety of important marine habitats including coral reefs, mangroves and sea grass beds (Rendon et al., 2022). These habitats are home to a number of highly endangered species such as the Irrawaddy dolphin, seahorses, dugongs and turtles. However, there are conflicting activities which have resulted in removal of mangroves and destruction of the sea grass beds as well as the first documented algal bloom in April 2016, which resulted in reduced tourist numbers. Some of these activities include electro-trawl fishing (much of which is illegal fishing) and removal of mangroves for construction of industrial areas, especially to the west of the region, where there is a new rice mill port, a new oil import port, and a new tourist port. Interspersed between these industrial ports are crab and squid fishing villages and activity areas. There are currently no water/wastewater treatment facilities in Kep province. With the assistance of a local NGO, Marine Conservation Cambodia, the local government aims to implement a zoning plan, but this has yet to take place. The provincial aim to have a "Clean City" that will promote tourist growth requires good water quality in the coastal marine environment. Scientific evidence is required to provide an understanding of the function of the various coastal habitats and how they can facilitate the maintenance of good water quality, and to decrease the risk of occurrence of harmful algal blooms which have negative impacts on the activities of the tourism sector.

## 2. Methods

### 2.1. Earth observations for environmental assessment

#### 2.1.1. Introduction

The key desirable characteristics for an EO dataset are precise and accurate measurement of the physical parameter in question, the ability to resolve small features, good coverage over a study area i.e. measurements where they are needed, long time series, and short repeat time between measurements. These characteristics are often in conflict. For example, high resolution sensors image a smaller area of the Earth for every satellite orbit, so record less frequently at any point. Stringent quality control results in fewer measurements and thus poorer coverage in time and space. For each of these datasets we have made a compromise to balance these characteristics. In the case of water quality measurements this has required multiple datasets, each with its own strengths and weaknesses.

#### 2.1.2. Sea Surface Temperature (SST)

For SST we have used NOAA's Pathfinder SST dataset (Casey et al., 2011) derived from measurements made by the AVHRR sensors. The AVHRR is a satellite radiometer that has flown on many satellites since 1978. While it offers a long time series the multiple sensors require inter-sensor biases to be accounted for. The Pathfinder dataset aims to debias these measurements and calibrate them against in-situ data.

The main limitations of this dataset are coarse resolution relative to some datasets derived from the visible spectrum, and few valid observations close to the coast due to contamination of the thermal signal from the sea by emission from the nearby land.

#### 2.1.3. Water quality

Water quality algorithms are based on water leaving reflectance whereas satellites measure top-of-atmosphere radiance. To convert from the latter to the former we must account for the absorption and scattering of radiation in the atmosphere and the sea surface and mask unwanted pixels corresponding to e.g. cloud.

For both chlorophyll and turbidity no algorithm excels everywhere as natural waters are highly optically diverse; the water itself, suspended sediment, dissolved organic matter, and phytoplankton all modify the reflected radiation. As an example, in the open sea where the optical properties of water are solely modified by phytoplankton and covarying substances, an algorithm based on the ratio of blue and green wavelengths is effective for measuring chlorophyll concentration. In coastal waters, dissolved organic matter absorbs blue light strongly, making blue/green ratios less effective, and algorithms targeting the near infrared can be preferable. For this reason we classify every water pixel in an image using "optical water types" (OWTs), where each water type is associated with the best performing algorithm in those conditions. We blend these algorithms to give the final dataset.

The basic steps used by all the water quality datasets are therefore:

1. Classify pixels with neural network and mask cloud, shadows etc.
2. Remove atmospheric effects to give water leaving reflectance
3. Identify optical water types for all water pixels
4. Use the best performing chlorophyll/turbidity algorithms for each OWT
5. Blend results from retrieval algorithms based on optical water type class membership

The water quality datasets are summarised in Table 1 and described in detail in the following sections.

**Table 1: Earth observation datasets used to assess water quality (chlorophyll and turbidity)**

| Dataset       | Variables                | Sensor                                  | Native nadir Resolution | Time series  | Advantages  | Disadvantages   |
|---------------|--------------------------|---|-------------------------|--|---|---|
| OC-CCI        | Chlorophyll              | SeaWiFS<br>MODIS<br>MERIS<br>(debaised) | 1 km                    | 09/1997-<br>07/2018                                      | + Long time series<br>+ High quality<br>away from coasts<br>+ Water focussed<br>sensors   | - Coarse<br>resolution<br>- Not focused on<br>optically complex<br>waters             |
| Calimnos 300m | Chlorophyll<br>Turbidity | MERIS<br>OLCI                           | 300m                    | 03/2003-<br>04/2012 (MERIS)<br>04/2016-present<br>(OLCI) | + Moderate<br>resolution<br>+ Water focussed<br>sensors<br>+ Optically<br>complex water<br>specific processor<br>+ Frequent revisit<br>time<br>+ Algorithm tuning<br>well constrained<br>by in-situ<br>measurements | - Moderate<br>resolution<br>- Shorter time<br>series<br>- Gap in time<br>series       |
| Calimnos 60m  | Chlorophyll<br>Turbidity | MSI                                     | 60m                     | 05/2015-present  | + High resolution<br>+ Optically<br>complex water<br>specific processor   | - Slower revisit<br>time<br>- Shorter time<br>series<br>- Land focussed<br>instrument |

#### 2.1.4. Chlorophyll a concentration at 1 km: Copernicus Climate Change Initiative: Ocean Colour (OC-CCI) (Sathyendranath et al., 2019)

As with the Pathfinder SST dataset this is a climate quality dataset. Reflectance data from the SeaWiFS, MODIS, and VIIRS sensors are “band shifted” to give a matching set of wavelengths across all the satellite missions and using the MERIS bands, and inter-mission biases are removed. Masking is stringent. (Lavigne et al., 2021). The use of older sensors gives a relatively long time series but limits the resolution of the dataset to 1 km. These factors limit its use around Da Nang Bay and Kep Province; however, we have included it here due to its long, climate-quality time series and stringent quality control.



### 2.1.4.1. Chlorophyll a concentration and turbidity processed with PML's Calimnos processor

PML's Calimnos processor is optimised for use for inland waters such as lakes and reservoirs. The ACCORD dataset is produced with the same methodology as the Copernicus Land Service's Lake Water Quality products (Copernicus, 2021a, 2021b). The optical water types and algorithms used are chosen for optically complex waters: those with high levels of suspended sediment, dissolved organic matter, and potentially very high chlorophyll concentrations. In addition, the satellite sensors used are relatively high resolution. This complements the OC-CCI dataset well: the Calimnos datasets are expected to perform best in near-shore and estuarine environments, whereas the OC-CCI datasets will perform better away from the shore.

### 2.1.4.2. 300 m dataset: Envisat MERIS and Sentinel 3 OLCI

MERIS is a multispectral sensor on the ENVISAT mission, with 300 m resolution, bands targeting spectral features useful for aquatic remote sensing, and high radiometric sensitivity (needed for aquatic remote sensing as the water signal is typically low). OLCI on the Sentinel 3 satellites is a follow on mission with similar characteristics. There are currently two Sentinel 3 satellites together giving repeat observations near-daily. There was a four-year gap between the missions so a continuous dataset is not possible. These data probably offer the best balance of resolution and algorithm performance for coastal remote sensing at present.

### 2.1.4.3. 60 m dataset: Sentinel 2 MSI

MSI is a multispectral sensor on the Sentinel 2 satellites (currently two in orbit). MSI was designed as a sensor for remote sensing of land targets. This means it lacks the high radiometric sensitivity of sensors designed for aquatic remote sensing, and has broad spectral bands meaning it cannot target the narrow spectral features used in some chlorophyll algorithms. We have included it here as it has 60 m resolution so can resolve smaller features. This is a good dataset for smaller features in Da Nang Bay.

## 2.1.5. Data access

All environmental described in this report are available in the PML data portal: <https://accord.eofrom.space/>

This is open access data portal, where data can be viewed and also basic plots can be made. Indicators (environmental variables) can be selected from the menu bar on the left hand side of the map. In the dropdown box "Show indicators sorted/grouped by:" choose "Region". The available indicators will then come up below this in dropdown menus for "Cambodia" and "Vietnam".

## 2.1.6. Statistical analysis

Time-series analysis: The regional minimum, maximum, mean, standard deviation and median values for each month for SST and chlorophyll were downloaded from the datasets in the data portal. For the larger scale (4 km and 1 km) datasets, the mean value was used in Minitab v18 with the Time Series

Decomposition analysis to separate the time series into linear trend, seasonal, and error components, using a multiplicative model.

Multivariate ENSO Index Version 2 (MEI.v2; <https://psl.noaa.gov/enso/mei/>) was also used to investigate for any correlations with large scale variables.

Regression analysis was carried out in Minitab v18 to investigate correlations between variables.

## 2.2. Earth Observations for mapping location of aquaculture sites

### 2.2.1. EO methods

Earth observation (EO) methods offer substantial benefits when applied to mapping and monitoring of the sea surface. They are more cost efficient compared to in-situ methods as large areas can be observed promptly on a regular basis. The observations use both the optical and microwave bands of the electromagnetic spectrum.

EO methods have been successfully applied for monitoring aquaculture structures, such as fish cages and floating houses, from space (Ballester-Berman et al., 2018; Ottinger et al., 2018; Stiller et al., 2019; Sun et al., 2020). However, this is a challenging task, mostly due to small sizes of these objects compared to sensor spatial resolution. For example, the resolution of Sentinel-1 SAR and Sentinel-2 MSI is comparable with the diameter of large circular floating net cages, which is about 10 meters, but is several times larger than the size of traditional wooden cages with typical rectangular frame length of 3 meters, used in Vietnam (Can and Tuan, 2012). Some commercial EO satellites, like QUICKBIRD or WORLDVIEW deliver images in high spatial resolution with pixel size less than 1 meter. However, application of high-resolution data is usually limited by their high cost and large time interval between repeated observations.

The resolution is not the only limiting factor of using EO data for mapping aquaculture structures from space. As the main structure of a fish cage is located underwater, only the top of the frame elements, made of wood, metal and plastic, may be mapped by the sensor. As the size of these objects is much smaller than sensor resolution and the optical reflectance properties are low, they can be hardly seen even in high resolution satellite data. As an example, Figure 2A shows a Google Map satellite image of fish cages at New Guinlo, Palawan, Philippines. The resolution of the image is about 0.4 meters and the cages can be clearly seen. For comparison, Figure 2B shows the Sentinel-2 MSI multispectral image of the same location with spatial resolution 10 meters and the fish cages are nearly impossible to see.

Microwave is more suitable for observing aquaculture structures, even at medium spatial resolution, as the wet wooden and bamboo components above the water surface, produce strong reflection of microwaves. This signal is clearly seen in the image when the water surface is relatively calm. For example, Figure 2C shows an image acquired by the Sentinel-1 synthetic aperture radar (SAR) sensor at C-band and dual polarizations (VV+VH). The bright spots in the middle of the image show the location of fish cages. The land is located at the right side of the image.

Several studies in the literature have successfully applied Sentinel-1 SAR for aquaculture: mapping aquaculture ponds in Vietnam (Ottinger et al., 2018; Sun et al., 2020), studying spatial-temporal patterns of coastal aquaculture in China (Stiller et al., 2019), spatial planning of finfish and shellfish aquaculture in

Spain (Ballester-Berman et al., 2018).

Here we use Sentinel-1 SAR images to map the location of aquaculture sites in Da Nang Bay and in Song-Cu-De and Hang rivers. This technique has been successfully applied in (Kurekin et al., 2022) for automated mapping of aquaculture sites in Palawan, Philippines. The study area and available satellite data are presented in Section 2.2.2. In Section 2.2.3 we describe the developed methodology for processing Sentinel-1 SAR sensor data and the processing chain to generate the aquaculture site maps.

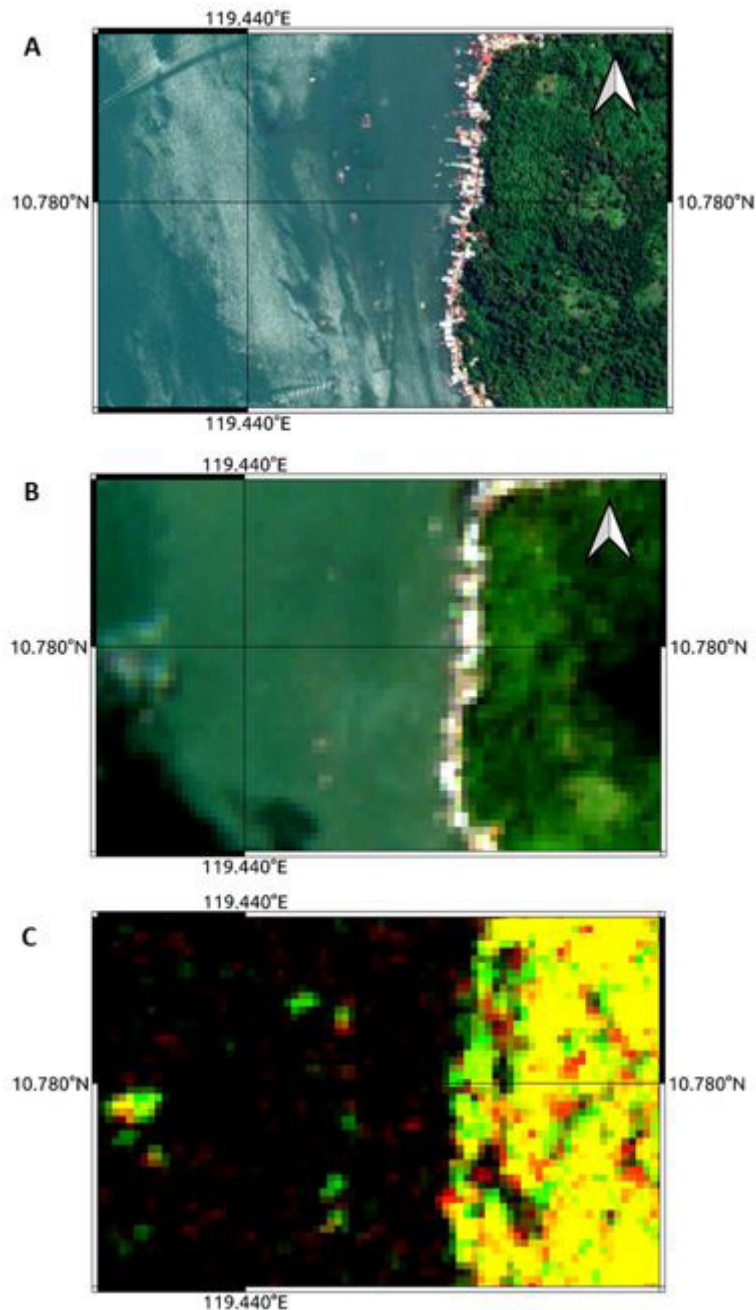


Figure 2. Fish cages in coastal waters of New Guinlo, Palawan, Philippines: A) Google Map satellite image; B) Sentinel-2 MSI sensor RGB image, resolution 10m; C) Sentinel-1 SAR sensor pseudo-colour image, resolution 20 m.

## 2.2.2. Study region and datasets

The study area is outlined in yellow in the map in Figure 3A. It includes the Da Nang Bay and the nearby rivers: Cu De, Song Du Toa, Cam Le and Hang, along with a coastal area South of Da Nang. The adjoining rivers are known for fish farming and aquaculture production (Tuan, 2003). Fish farming was developing in this location through a local pilot program that started in 2000. After a mass fish mortality event in summer 2017 the local government introduced a ban on aquaculture. Despite the financial losses estimated in millions of dong and the absence of financial help from the local government, the farmers still continue growing fish in cages and according to (Xuan, 2018), several dozens of fish cages can still be found in the rivers Co Co and Han.

To map aquaculture sites in Da Nang Bay we used Sentinel-1A SAR data . The main benefits of using SAR sensor for this region, known for dense cloud cover for most of the year, are the all-weather day and night observation capabilities. Currently, only the Sentinel-1A SAR is scheduled to operate over Da Nang Bay and the data from Sentinel-1B sensor are not available for this region. The location of image granule coverages available for the study region are shown in Figure 3B, where the ascending passes are outlined in red and descending are outlined in blue. The revisit time interval for both ascending and descending passes varies from 4 to 8 days. Over the study area the sensor operates in the interferometric wide swath (IW) mode and delivers images of the Earth surface using vertical transmit vertical receive (VV) and vertical transmit horizontal receive (VH) polarisations and at spatial resolution 5 by 20 meters. At Level 1 the satellite images are available in two formats: Single Look Complex (SLC) product that includes complex samples at resolution 5x20 meters; and high-resolution ground range detected (GRDH) product that contains multi-look samples at reduced spatial resolution 20x20 meters.

For the task of aquaculture site mapping we used the SLC product, which has 4 times higher spatial resolution along the sensor range axis. However, the level of speckle noise in the SLC data is much higher compared to the GRDH product that combines several independent measurements to reduce speckle (Ulaby et al., 1982). Speckle is a well-known phenomenon that degrades the quality of SAR images. It is produced by random interferences of a set of coherent wave-fronts and appears as grainy structure in SAR images.

Due to the small size of aquaculture objects, their contrast in SAR images is relatively low and it is important to reduce speckle to improve discrimination of such objects. This cannot be achieved by standard methods based on speckle filtering techniques as the size of fish cage in satellite images does not exceed several pixels. A special technique has been developed to reduce speckle noise in SLC product, which is described in Section 2.2.3.

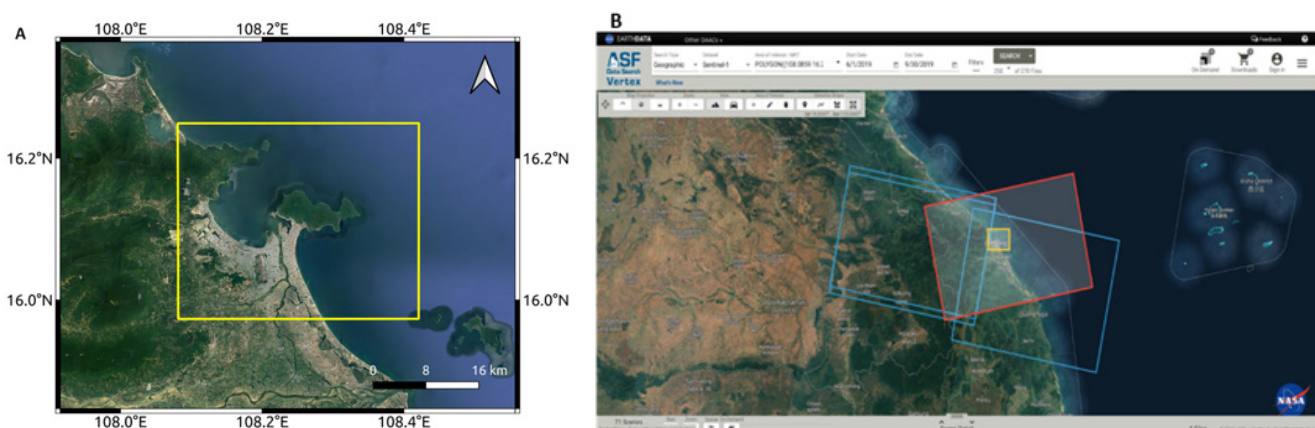


Figure 3. The map of study area: A) the outline of aquaculture site map (in yellow); B) Sentinel-1A sensor ascending scenes, outlined in red; descending scenes, outlined in blue.

### 2.2.3. Methodology and data processing chain

The aquaculture structures, such as finfish cages, shellfish farms or jetties and floating houses for servicing aquaculture sites, are static objects that do not change their position over long period of time. This property has been used to solve two main problems: reduction of speckle noise in SAR images without loss of spatial resolution; discrimination of aquaculture structures from ships and boats that have similar size and appearance in Sentinel-1 SAR images. Both problems were resolved by using the same approach, which consists of: processing time series of SAR images over relatively large time interval; integrating processed data into one composite image; and finally, generating a map of static objects. The composite image is generated by applying a median operator to all pixels in the image along the time dimension. The median operator is often used as a noise filtering technique and allows reduction of speckle noise in the composite image. It is also known for its property to remove outliers in the input data. We used this feature to discriminate moving objects in SAR images, such as ships and boats. In the time series of SAR images these dynamic objects change their position and can be considered as spikes along the time axis.

The main processing steps are shown in the flow-chart in Figure 4. The processing chain in Figure 4 consists of several stages. Firstly, the Sentinel-1A SAR scenes are selected covering the specific time interval and geographic area. The selected SAR data are then downloaded from the Alaska Satellite Facility Archive (ASFA), stored and then passed to the next processing stage. During this stage the radiometric calibration is performed to convert SLC product data to the absolute normalized radar cross section (NRCS) values. Then, the algorithm called "Terrain Observation with Progressive Scans SAR (TOPSAR) De-burst and Merge" (De Zan and Guarnieri, 2006) is applied to combine several sub-swath images and individually focused complex burst images into a single image. This is followed by converting SLC data that preserve both the amplitude and phase information, into an amplitude image. Then, the image is mapped into the geographical coordinates of a study region.

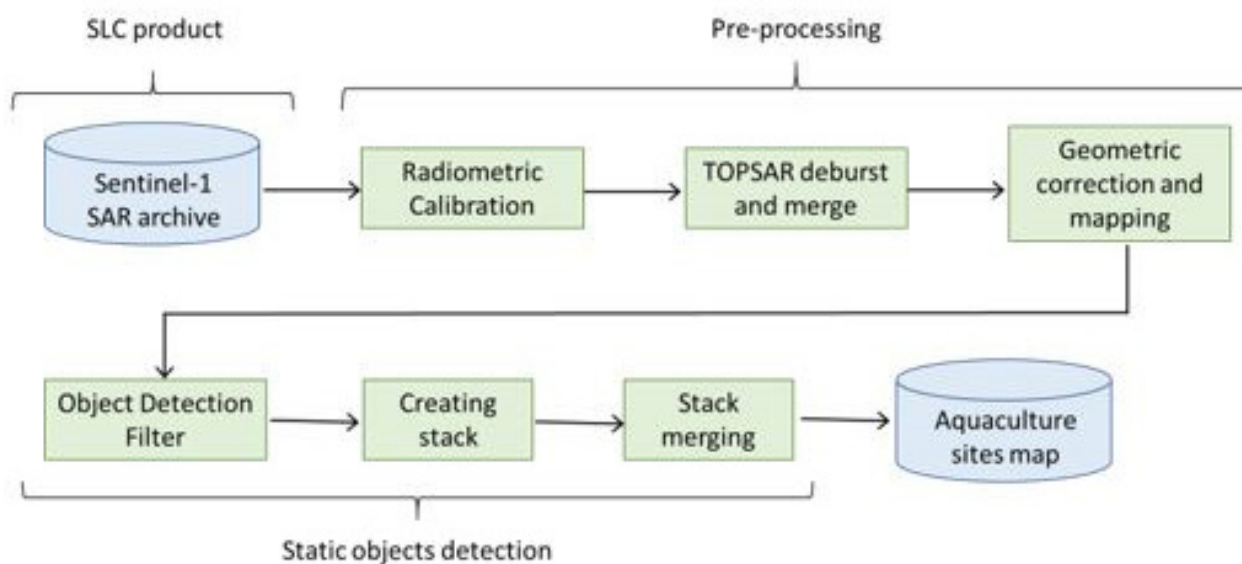


Figure 4. The Sentinel-1 SAR data processing chain.

Figures 5A-B show the examples of SLC data after preliminary processing. An aquaculture site is located in the middle of the image. The fish cages, scattered around the site, can be seen as bright spots simultaneously at VV and VH polarizations.

At the next stage we combine all pre-processed scenes into a single composite image that shows the

location of static objects. To discriminate small objects in the scene from the background, we apply a sliding window contrast box filter (Crisp, 2004) with the background window size 300 meters, guard window size 60 meters and target window size 1.5 meters. This filter adapts to the image background of varying intensity and discriminates small bright objects, such as ships and fish cages. An example of the image processed with contrast box filter is shown in Figure 5C-D. It is seen that the filter emphasized the objects in the centre of the image and suppressed the background noise.

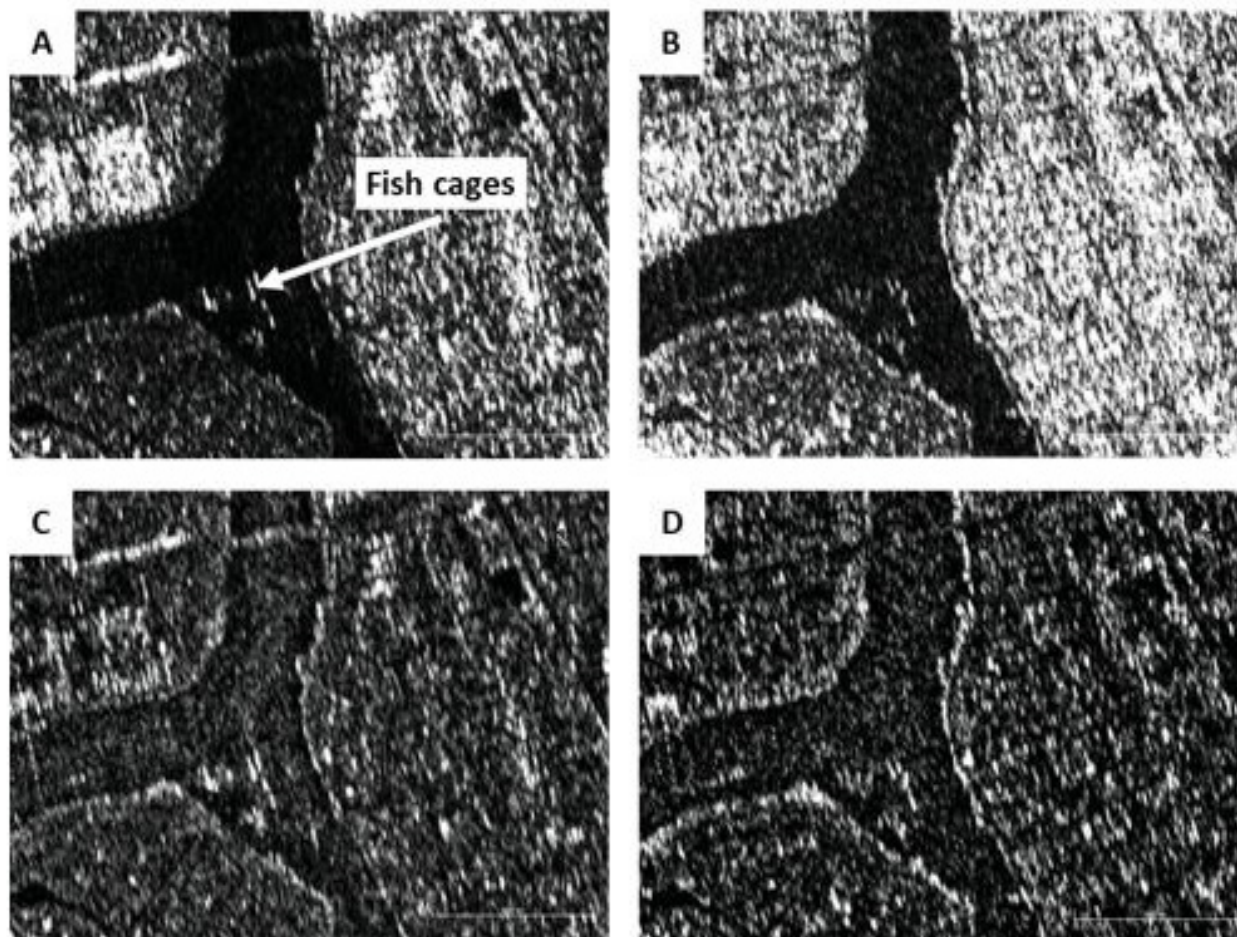


Figure 5. Sentinel-1A SAR data at different processing stages: A) VV-polarization and B) VH-polarization images after TOPSAR de-burst and geometric correction; C) VV- and D) VH-polarization data at the output of object detection filter. The location of aquaculture site is indicted with an arrow.

After processing all scenes with the contrast box filter the data are stacked into a three-dimensional array with two dimensions linked to the geographical coordinates and the third dimension associated with time (see Figure 4). The composite image is generated by calculating sample median along the time dimension. An example of a composite image is shown in Figure 6A The VH-polarisation in the RGB image in Figure 6 is shown in red, VV-polarisation is shown in green and blue channel is set to zero.

The relationship between VV- and VH-polarisations in Figure 6 is indicated by the changing colour of the image: objects characterised by strong backscattering at VV polarisation are shown in green and objects with strong VH-polarisation component are shown in pink. The objects with strong backscatter at both VV- and VH-polarisations are shown in yellow. The water in Figure 6 is shown in black as it is a smooth surface compared to the land and the backscatter from water surface is relatively weak. The bright spots on the water show the location of static objects only and all moving objects (ships, boats) are not visible in the image as they were suppressed by the median operator.

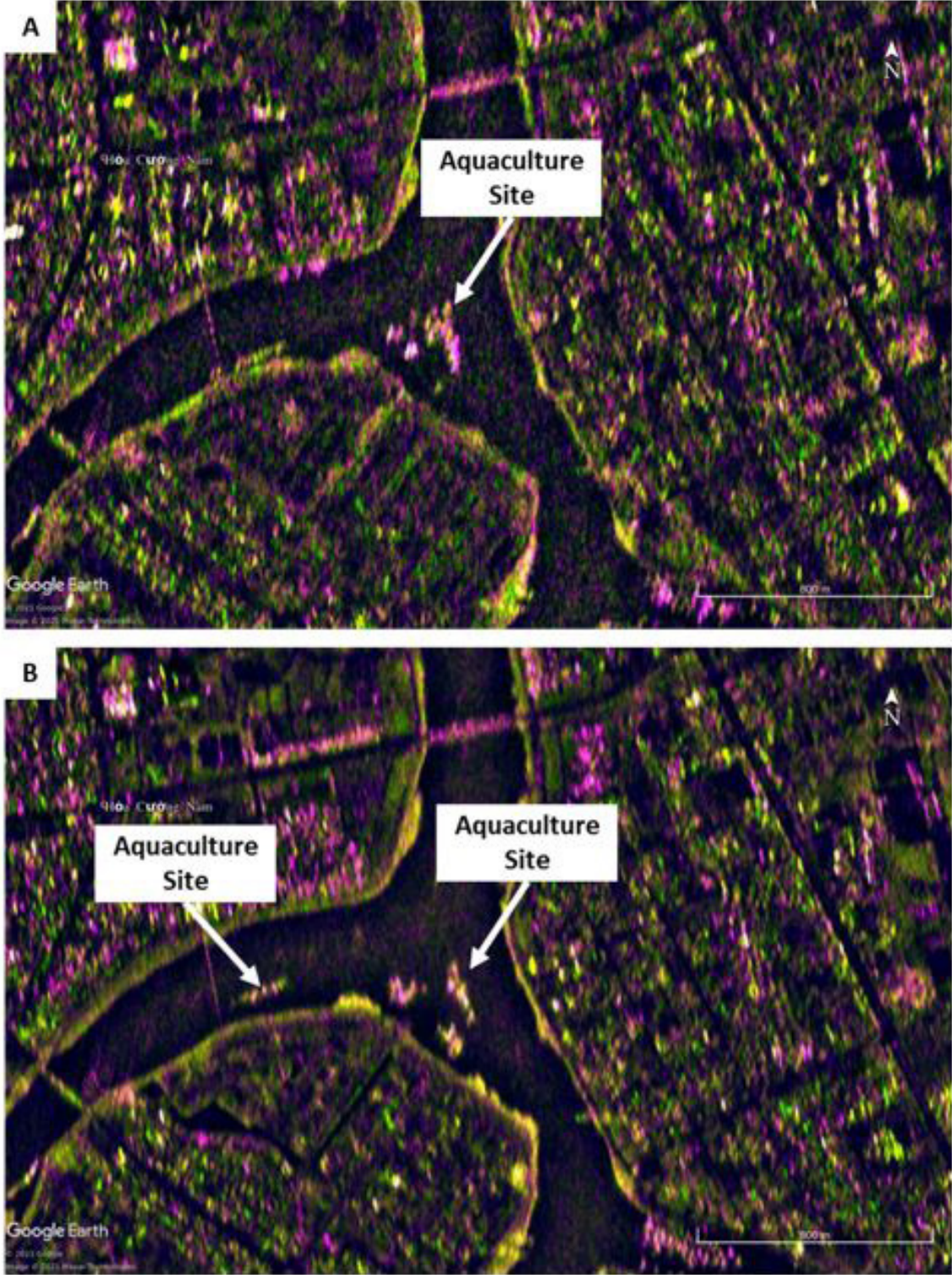


Figure 6. A map of aquaculture site at river Chan Do: A) in year 2017; B) in year 2019.

## 3. Results

### 3.1. Vietnam environmental assessment

#### 3.1.1. Large scale regional analysis (13 – 19 °N; 106 – 112 °E)

The time series decomposition showed a good fit between model and data (MAPE = 1.69%, MAD = 0.456, MSD = 0.346). Regionally averaged SST showed clear seasonal dynamics, with lowest mean temperature (~24 °C) occurring between December and February in the wet season, and highest mean temperature (~30 °C) occurring in the dry season, peaking in August and September (Figure 7). There was no significant linear trend through time in regionally averaged SST data, when seasonality was removed ( $r^2 = 0.0035$ ,  $F_{df=253} = 0.89$ ,  $p = 0.346$ ).

The time series decomposition for OC-CCI chlorophyll a also showed a good fit between model and data (MAPE = 13.01%, MAD = 0.031, MSD = 0.002). As with SST, the regionally averaged chlorophyll a showed clear seasonal dynamics; however, these dynamics were inverse to SST, such that the lowest chlorophyll a levels occur during the dry season, and highest levels occur during the wet season (Figure 7). There is a strong significant negative correlation between SST and chlorophyll a ( $r^2 = 0.4887$ ,  $F_{df=245} = 233.21$ ,  $p < 0.0001$ ), whereby, statistically, about 50% of the variability in chlorophyll a can be explained by the variability in SST, despite SST and Chlorophyll a data having different spatial resolutions (4 km vs 1 km). The time series analysis shows that there is a weak but significantly positive linear trend through time in the regionally averaged chlorophyll a data, when seasonality was removed ( $r^2 = 0.06$ ,  $F_{df=249} = 15.83$ ,  $p < 0.0001$ ,  $\alpha = 0.00004$ ).

The MEI did not appear to have strong relationships with either regionally averaged SST or chlorophyll a, although there was significant correlations with the deseasonalised data (SST:  $r^2 = 0.062$ ,  $F_{df=253} = 16.57$ ,  $p < 0.0001$ ,  $\alpha = 0.1503$ ; Chl:  $r^2 = 0.016$ ,  $F_{df=249} = 3.98$ ,  $p = 0.047$ ,  $\alpha = 0.00493$ ).

Spatially, the majority of the chlorophyll a occurs along the coast to about 50 km offshore (Figure 8) and sometimes extending across the shelf. Off shelf there is very low chlorophyll a levels year-round. The coastal chlorophyll a peaks often correlate to a tongue of cooler water that forms along the coast especially during the wet season (Figure 8A-B), which likely corresponds to increased river run off during that season. During the dry season, SST is more uniform across the region, as is the low chlorophyll a levels (Figure 8C-D).



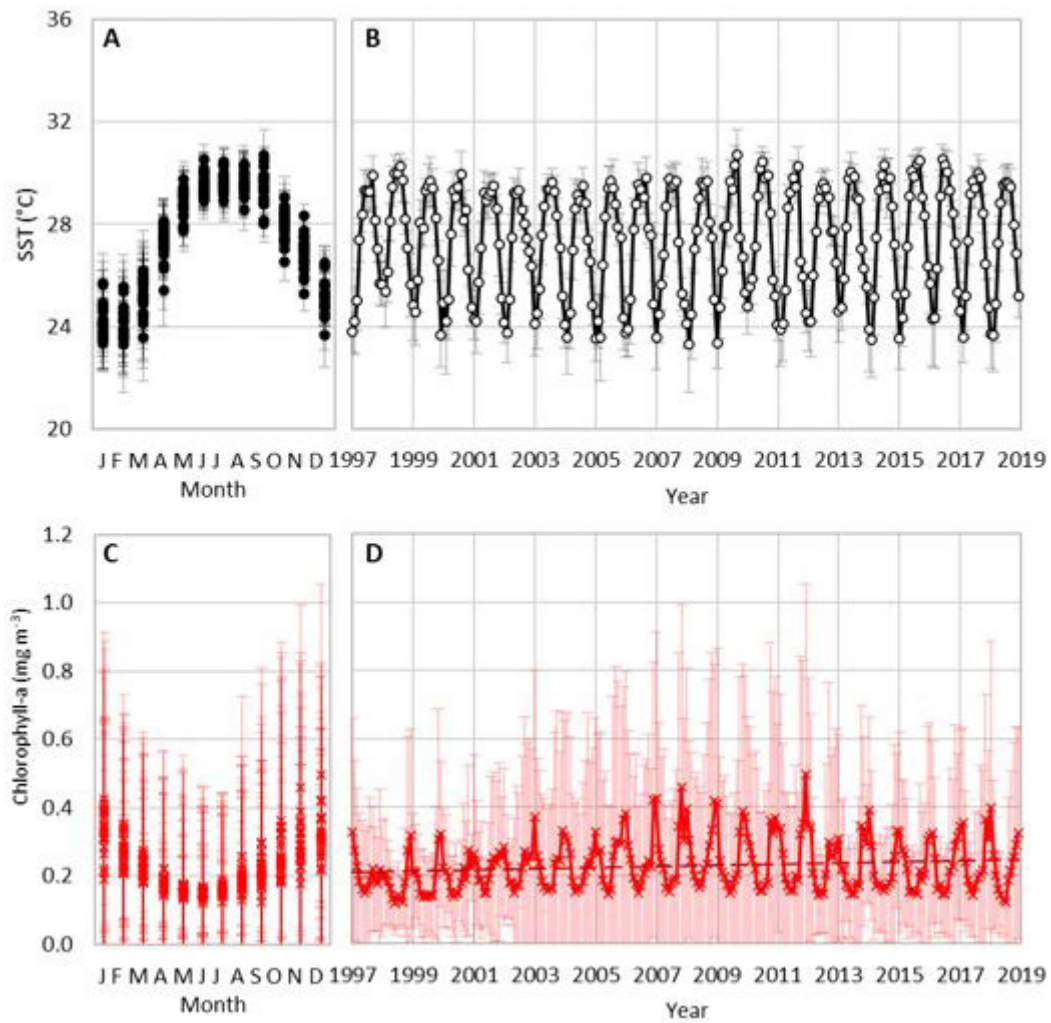


Figure 7: Vietnam regionally averaged monthly NOAA's Pathfinder surface temperature (SST) (A & B) and OC-CCI chlorophyll a concentration (C & D). Seasonal cycles are presented in A & C and full time-series is presented in B & D. Circles and crosses represent the mean values, error bars represent the standard deviation. The red dashed line in D shows the linear trend through time for chlorophyll a.

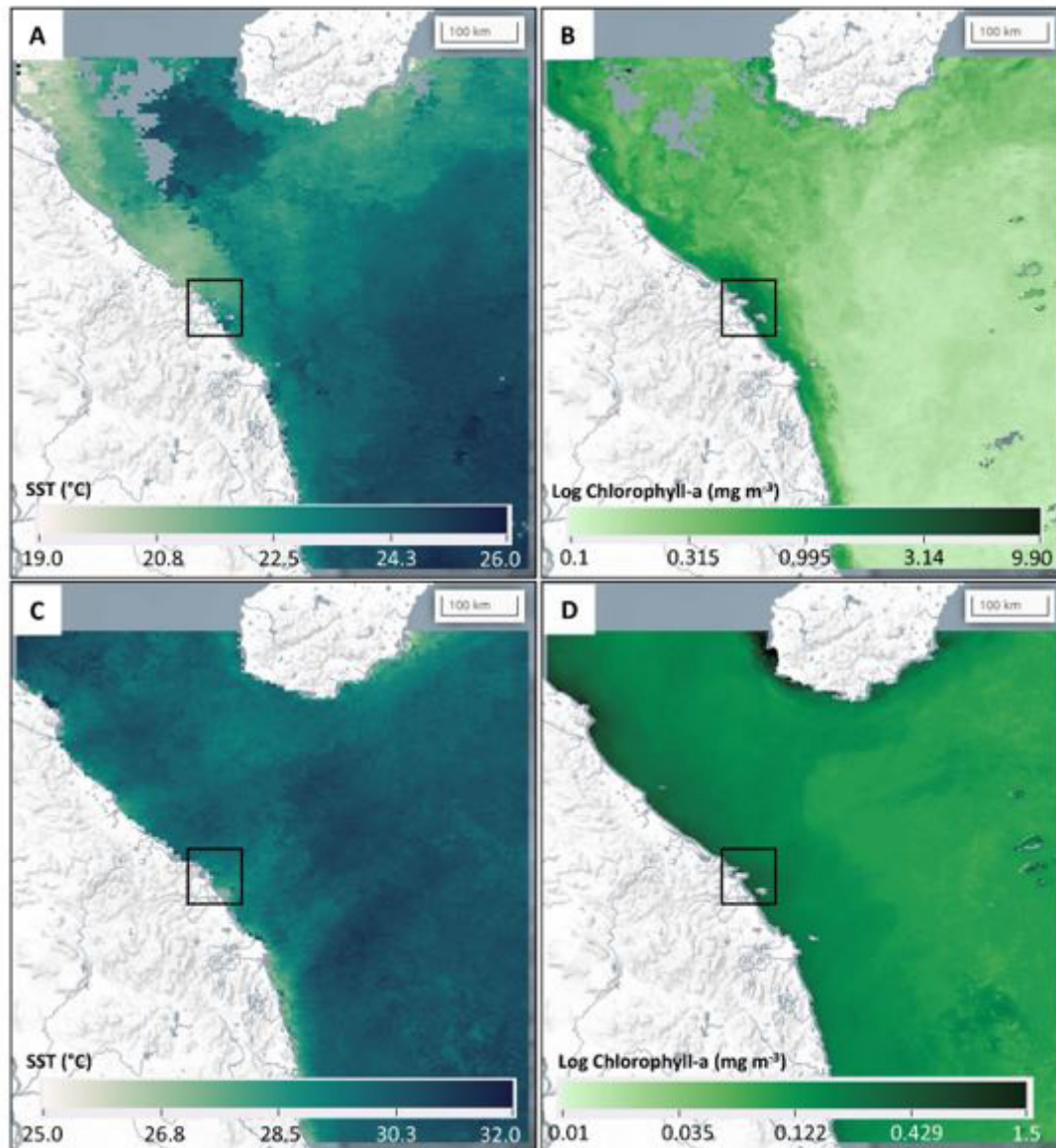


Figure 8: Earth Observation images for NOAA's Pathfinder sea surface temperature (A & C) and OC-CCI chlorophyll a concentration (B & D) showing monthly composites for January (A & B) and June (C & D). Note that the images are presented on different scales. The black box shows the region around Da Nang Bay.

### 3.1.2. Da Nang local analysis (300 m & 60 m datasets)

The high resolution Calimnos datasets, both the 300 m and 60 m, provide much more detail around the Da Nang bay area. In the 300 m dataset, high chlorophyll can be observed nearshore all year around, especially around the mouth of the Hàn River on the south east side of Da Nang bay, and outside the bay around Lap An Lagoon and Chan May Bay. This high chlorophyll could represent blooms or could be an impact of sediments. Chlorophyll concentrations are strongest in the winter months (e.g. November 2019 shown in Figure 9A). The 60 m dataset provides significantly more detail within Da Nang bay, showing the high chlorophyll levels are actually more local than implied by the 300 m dataset, and especially most prominent features around the mouth of the Hàn River (e.g. November 2019 shown in Figure 9B). The higher chlorophyll a levels observed elsewhere along the coast in the 300 m dataset are not significant features in the 60 m chlorophyll dataset.

A similar level of detail can be found in the turbidity datasets from the 300 m and 60 m product. Turbidity levels are greatest in the very nearshore especially through the winter months during the wet season (e.g. November 2019 shown in Figure 10A). In the example of November 2019, a high turbidity feature can be seen in the middle of Da Nang Bay. The 60 m dataset displays this feature much more clearly, showing it linking the flows out of the two main rivers (the Song Cu De to the west and the Han River to the east). There appears to be a closer match between the 300 m and 60 m datasets in general, compared to the chlorophyll datasets, whereby higher turbidity levels seen in the 300 m dataset are usually also apparent in the 60 m dataset.

The Calimnos 60 m turbidity dataset can be used to highlight interesting hydrodynamic features around Da Nang bay. Figure 11 demonstrates a few examples: Figure 11A shows turbidity for January 2016, while Figure 11B shows turbidity for August 2016. Arrow 1 points out an eddy to the south of Hai Son Cha Island which is present in January but not present in August; instead there is northward movement between the island and the mainland peninsula. The change in flow within and around the bay is also notable from the plume of higher turbidity coming from the rivers moving west and north in January but moving east and north in August. Arrow 2 points out large turbidity features in January 2016 offshore from My Khe Beach in the south. Arrow 3 highlights another eddy feature off the southern peninsula. This features in August 2016 can also be seen as higher chlorophyll a concentrations.

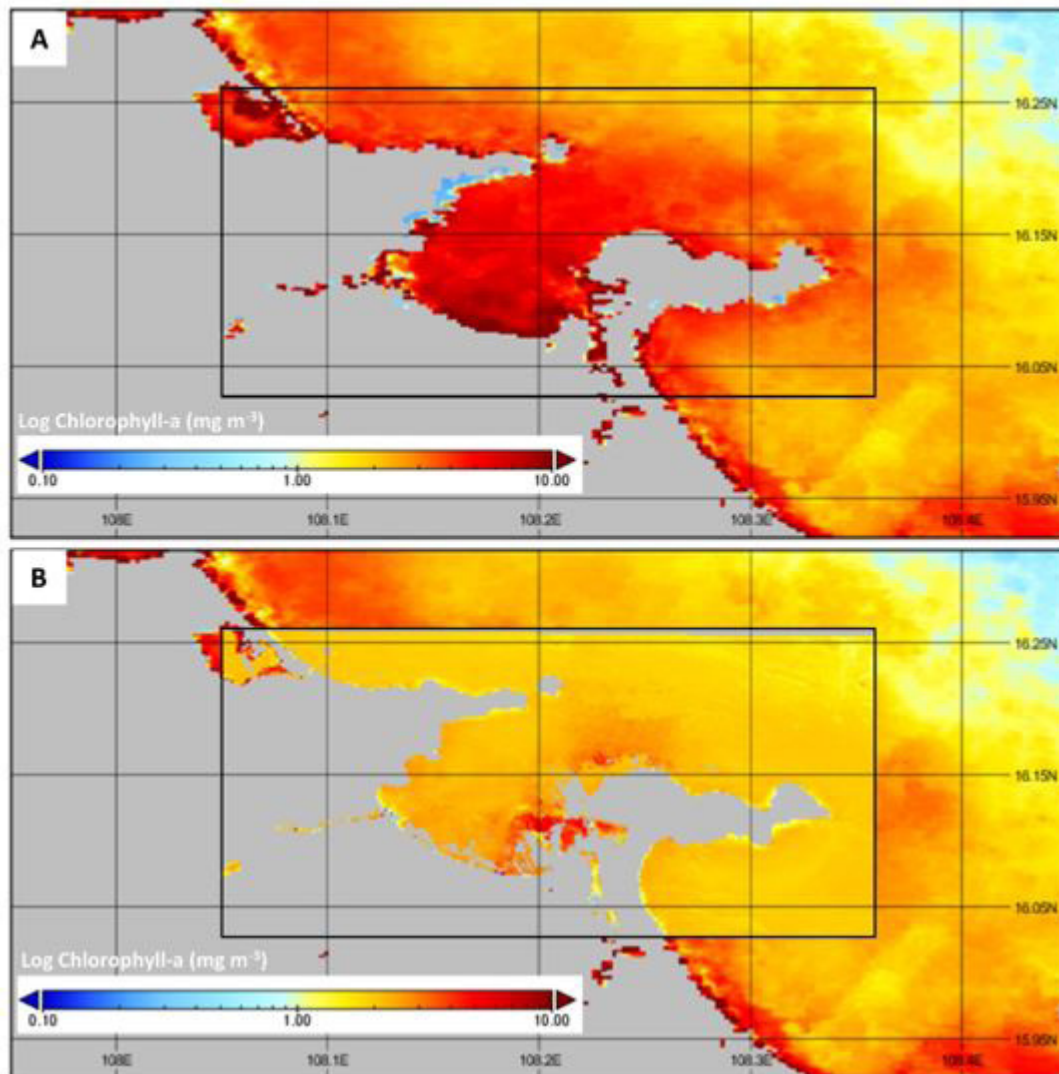


Figure 9: Comparison between the Calimnos 300 m chlorophyll a concentration dataset (A) and the Calimnos 60 m chlorophyll a concentration dataset (B) inset on top of Calimnos 300 m. Example of monthly composite from November 2019. The box highlights the area covered by the 60 m dataset.

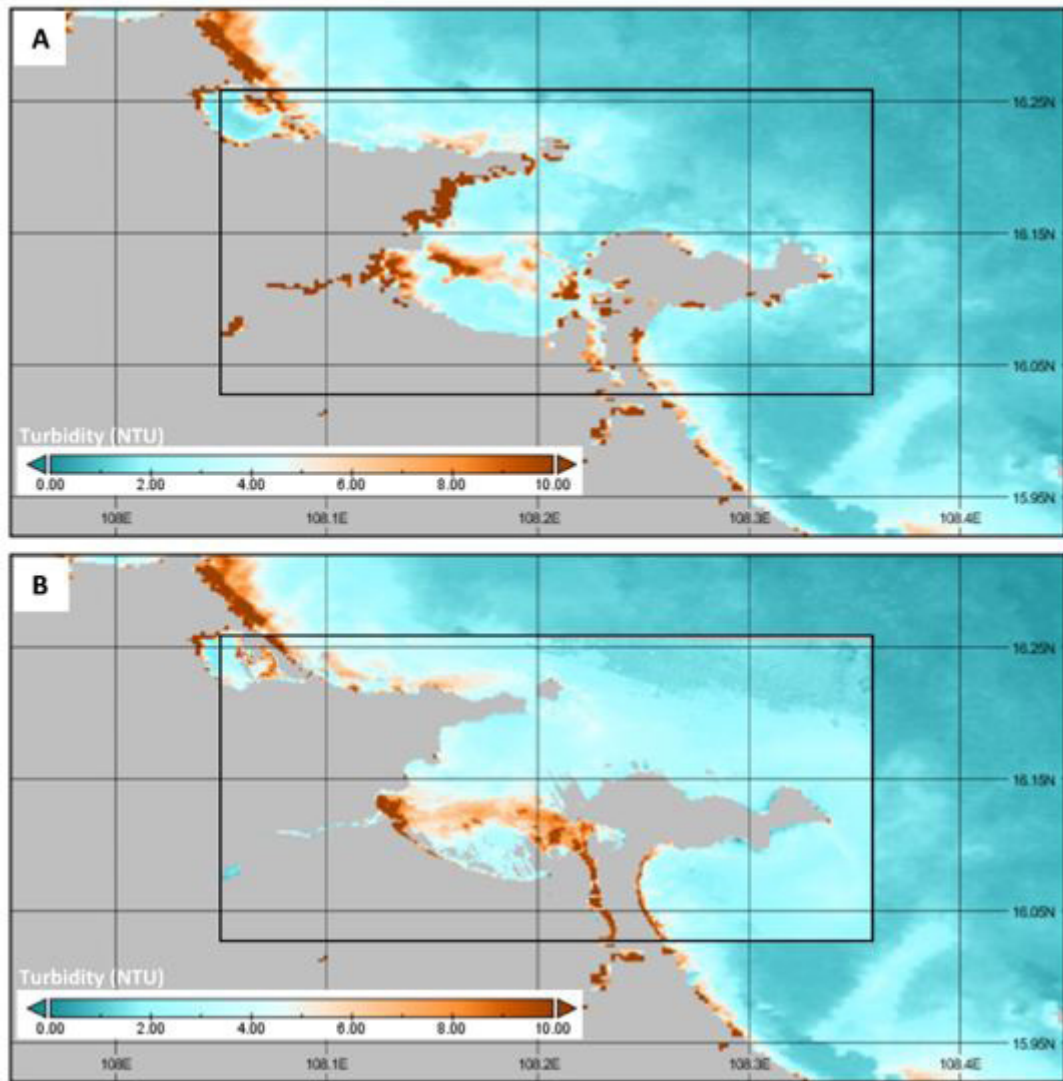


Figure 10: Comparison between the Calimnos 300 m Turbidity dataset (A) and the Calimnos 60 m Turbidity dataset (B) inset on top of Calimnos 300 m. Example of monthly composite from November 2019. The box highlights the area covered by the 60 m dataset.

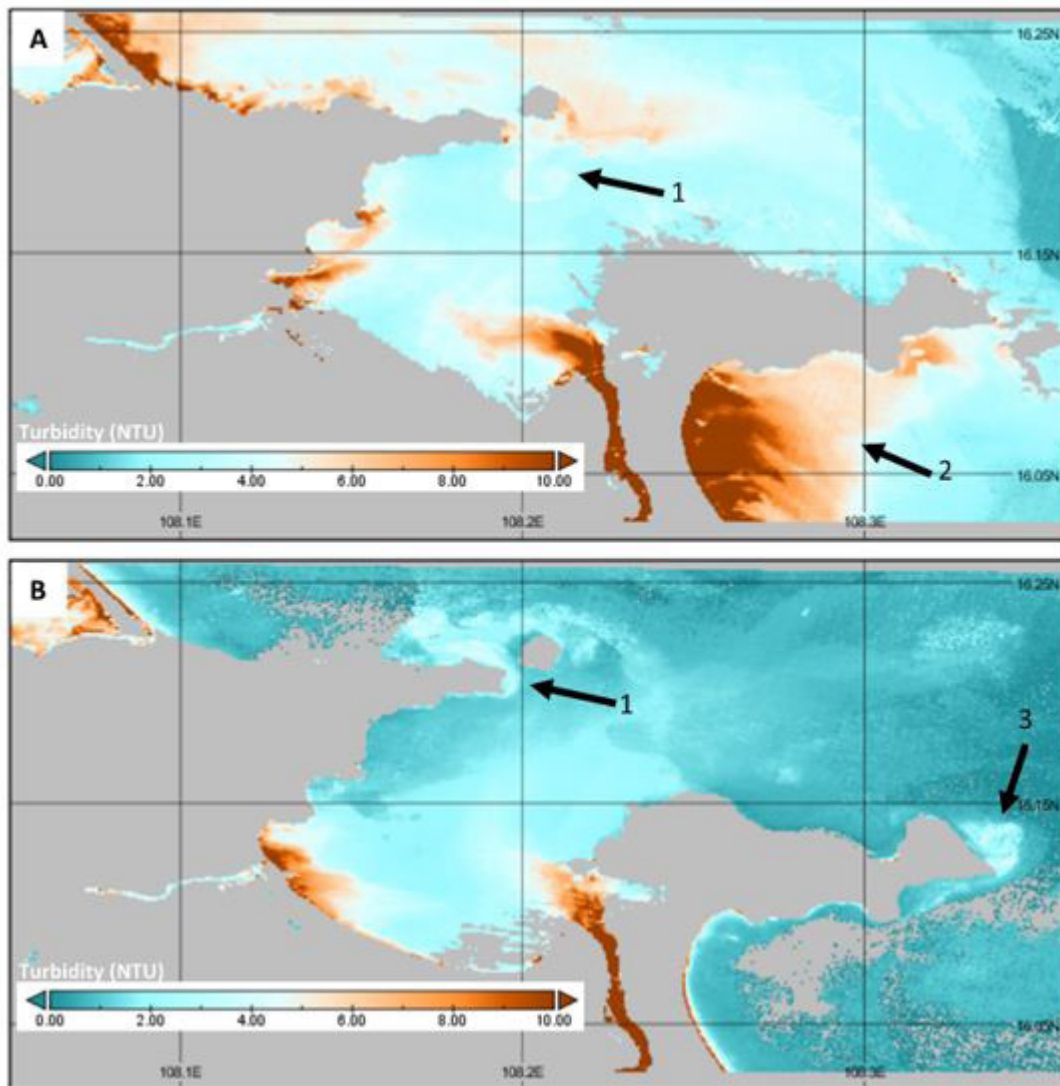


Figure 11: Calimnos 60 m turbidity dataset showing monthly composites for January 2016 (A) and August 2016 (B). Arrows highlight three examples of hydrodynamic features. See text for details.

## 3.2. Cambodia environmental assessment

### 3.2.1. Large scale regional analysis (9 – 11 °N; 103 – 105 °E)

The time series decomposition showed a good fit between model and data (MAPE = 1.65%, MAD = 0.484, MSD = 0.384). Regionally averaged SST showed clear seasonal dynamics, with lowest mean temperature (~27 °C) occurring between December and January, and highest mean temperature (~32 °C) peaking in April and May (Figure 12). These peaks fall just before the rainy season, which is considered to occur between May and November. There was no significant linear trend through time in regionally averaged SST data, when seasonality was removed ( $r^2 = 0.0062$ ,  $F_{df=244} = 1.52$ ,  $p = 0.219$ ).

The time series decomposition for OC-CCI chlorophyll a also showed a good fit between model and data (MAPE = 9.74%, MAD = 0.070, MSD = 0.010). As with SST, the regionally averaged chlorophyll a showed clear seasonal dynamics, with levels peaking in September, but generally high through the rainy season, and lowest in March and April (Figure 12). These dynamics did not correlate with SST ( $r^2 = 0.043$ ,

Fdf=236 = 1.01,  $p=0.317$ ). There was no trend through time in the regionally averaged chlorophyll data, when seasonality was removed ( $r^2 = 0.017$ , Fdf=250 = 0.43,  $p=0.514$ ).

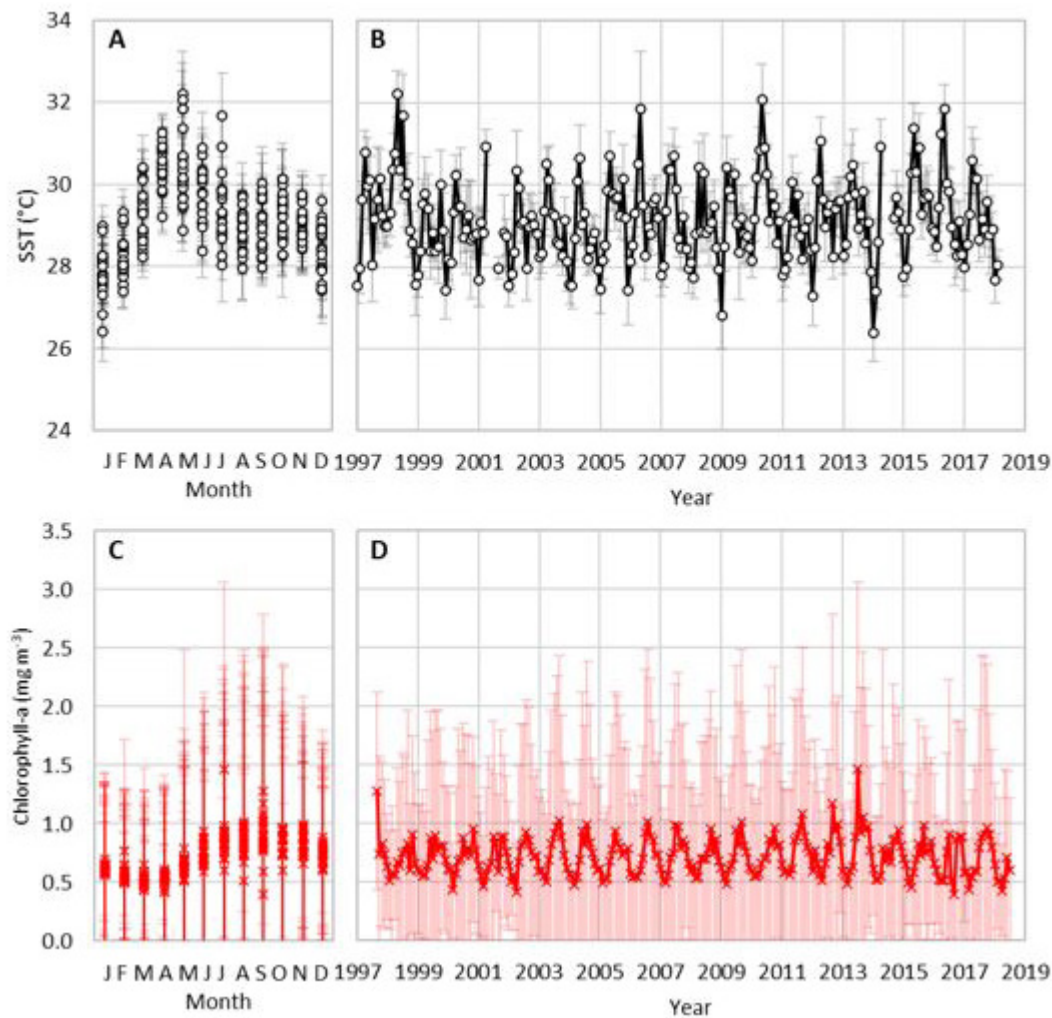


Figure 12: Cambodia regionally averaged monthly NOAA's Pathfinder sea surface temperature (SST) (A & B) and OC-CCI chlorophyll a concentration (C & D). Data are presented in seasonal cycles (A & C) and full time-series (B & D). Circles and crosses represent the mean values, error bars represent the standard deviation.

The MEI had a weak but significant correlation with regionally averaged deseasonalised SST but not chlorophyll (SST:  $r^2 = 0.074$ , Fdf=244 = 19.32,  $p < 0.0001$ ,  $\alpha = 0.1660$ ; Chl:  $r^2 = 0.0002$ , Fdf=250 = 0.06,  $p = 0.804$ ).

Spatially, the main chlorophyll peak occurs nearshore (Figure 13A), and especially in the southeast across the Vietnamese border, in the Vịnh Rạch Giá area where there appears to be significant agricultural and aquaculture activity, as well as canals that connect to the Bassac River and Sông Hậu Giang.

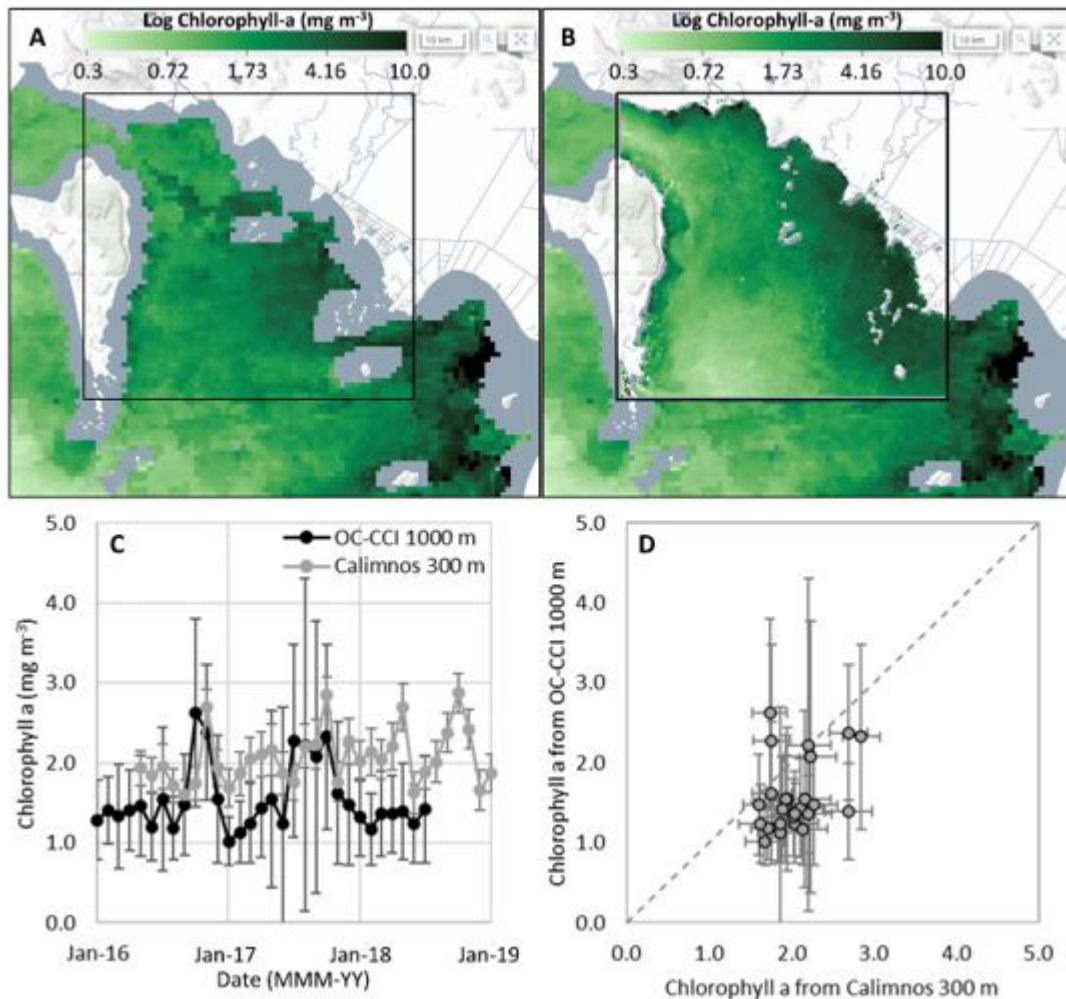


Figure 13: Comparison between the OC-CCI (1 km) chlorophyll a concentration dataset (A) and the Calimnos (300 m) chlorophyll a concentration dataset (B), visual example from October 2017. The inset box highlights the area covered by the Calimnos dataset. Regionally averaged chlorophyll a concentration for both datasets, from the same areal extent, is shown in (C) as mean and standard deviation (error bars), and compared against each other in (D).

### 3.2.2. Kep province local analysis (300 m resolution)

To make an assessment of the usefulness of the 1000 m OC-CCI Chlorophyll a dataset in the Kep Province we compared monthly regionally averaged data from overlapping time periods with 300 m resolution chlorophyll a dataset using the same areal extent (Box 103.992 °E , 9.971 °N, 104.653 °E, 10.601 °N; Figure 13). This comparison shows that on average, the same seasonality is picked up in both datasets, but the finer resolution data gives slightly higher values on average because it is detecting near shore concentrations, which tend to be higher than offshore.

The suspended sediment dataset highlights the influence of rivers in determining water quality of the region. Spatially, the suspended sediment concentration is greatest along the coast, and is greatest during the rainy season, with sediment flowing out of the major river channels. Figure 14 highlights the particularly high levels of suspended sediment in 2018, especially flowing out of the Preaek Tuek Chhu river near Kampot in the north of the region, and Giang Thanh River in Vietnam to the south of the region (both areas are marked on Figure 14 with red boxes). Sediment from the north, can, in some months move along the coast towards the Kep National park area, while sediment from the south tends

to move to the east and north, towards the islands in the central bay. The highest sediment loads do not correlate with high chlorophyll a concentration. It is likely that these high sediment loads prevents enough light from allowing large blooms to occur. However, there is generally higher chlorophyll a concentration in areas near the coast and in the shallow bay region between the mainland and the small islands within the bay. In October 2018 there is a large bay-wide peak in chlorophyll, possibly enhanced by the high river loads in the months prior bringing higher nutrient conditions (Figure 14K).

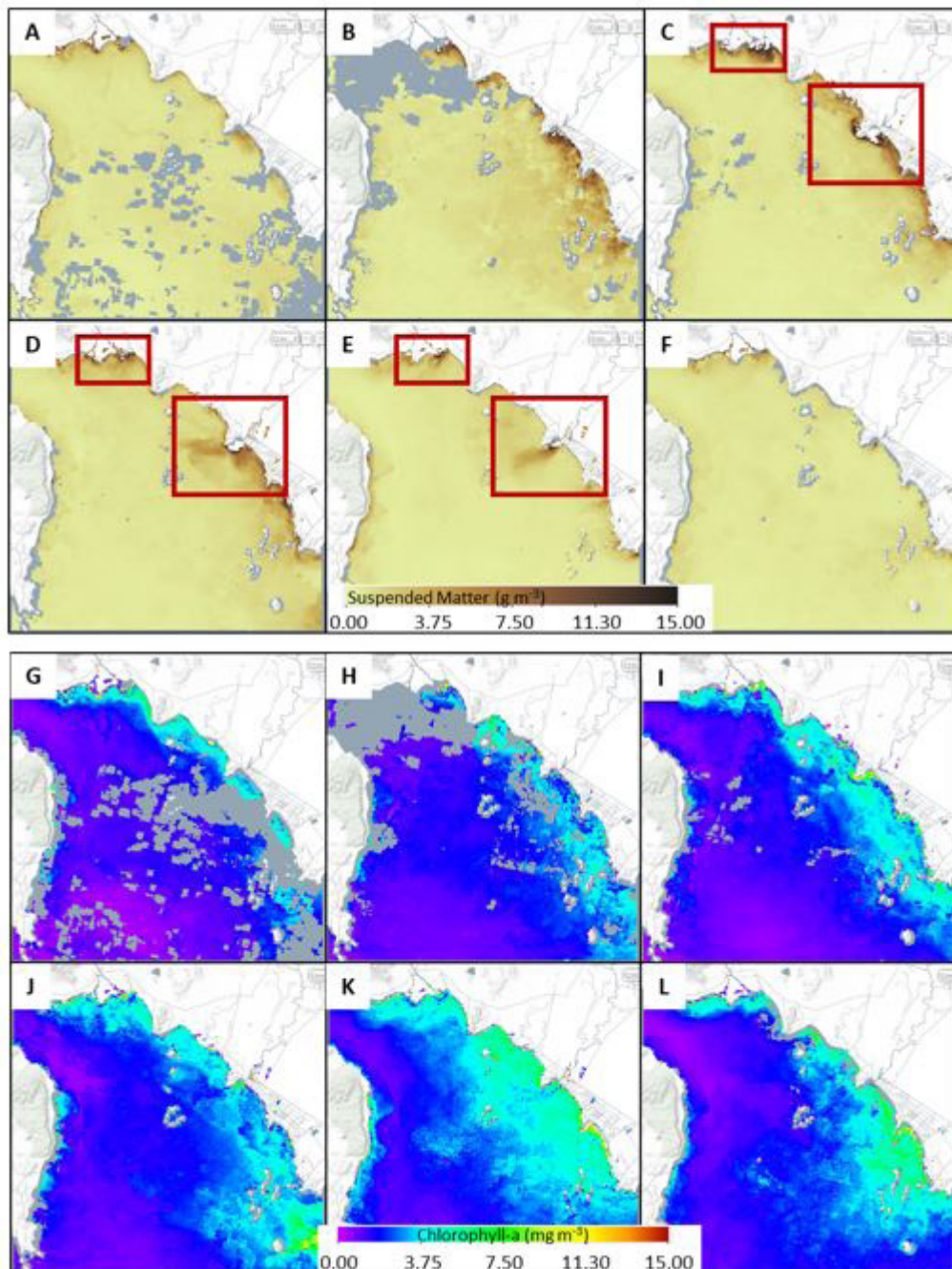


Figure 14: Earth Observation images from the Calimnos 300 m dataset for suspended sediment representing monthly composites June – November (A – F) for year 2018, and chlorophyll a concentration monthly composites June – November (G – L) for year 2018. Red boxed highlight areas of high sediment load.



### 3.3. Da Nang aquaculture assessment

The methodology presented in Section 2.2 has been applied to generate a map of static objects, such as fish cages and shellfish farms. Two maps were generated in years 2017 and 2019 by processing and compositing Sentinel-1A SAR scenes over the period from June to September in these years. The total number of processed scenes was equal to 20 in 2017 and 24 in 2019. Figure 3B illustrates the spatial coverage of the study area by Sentinel-1A sensor. The four-month time interval over which the satellite images were combined, was considered sufficiently long to reduce the speckle noise and suppress moving objects, but also short enough to retain static objects in the composite image. The generated composite map of aquaculture objects is shown in Figure 15. The map is presented in RGB colour format with VH-polarisation shown in red and VV-polarisation shown in green. An enlarged fragment of the map is presented in Figure 6. It shows river Cau-Do and the aquaculture site in the middle of the scene along riverbank.



Figure 15: The Sentinel-1 SAR map of static objects, such as fish cages and shellfish farms in year 2019.

The dark areas in the figure correspond to the water and bright blobs show the location of aquaculture structures. Figure 6 illustrates the changes of aquaculture sites from 2017 to 2019. The comparison of the maps in Figure 6A and Figure 6B shows that the number of fish cages has changed over time and a new aquaculture site was created at river Cau-Do to the West of the first site location.

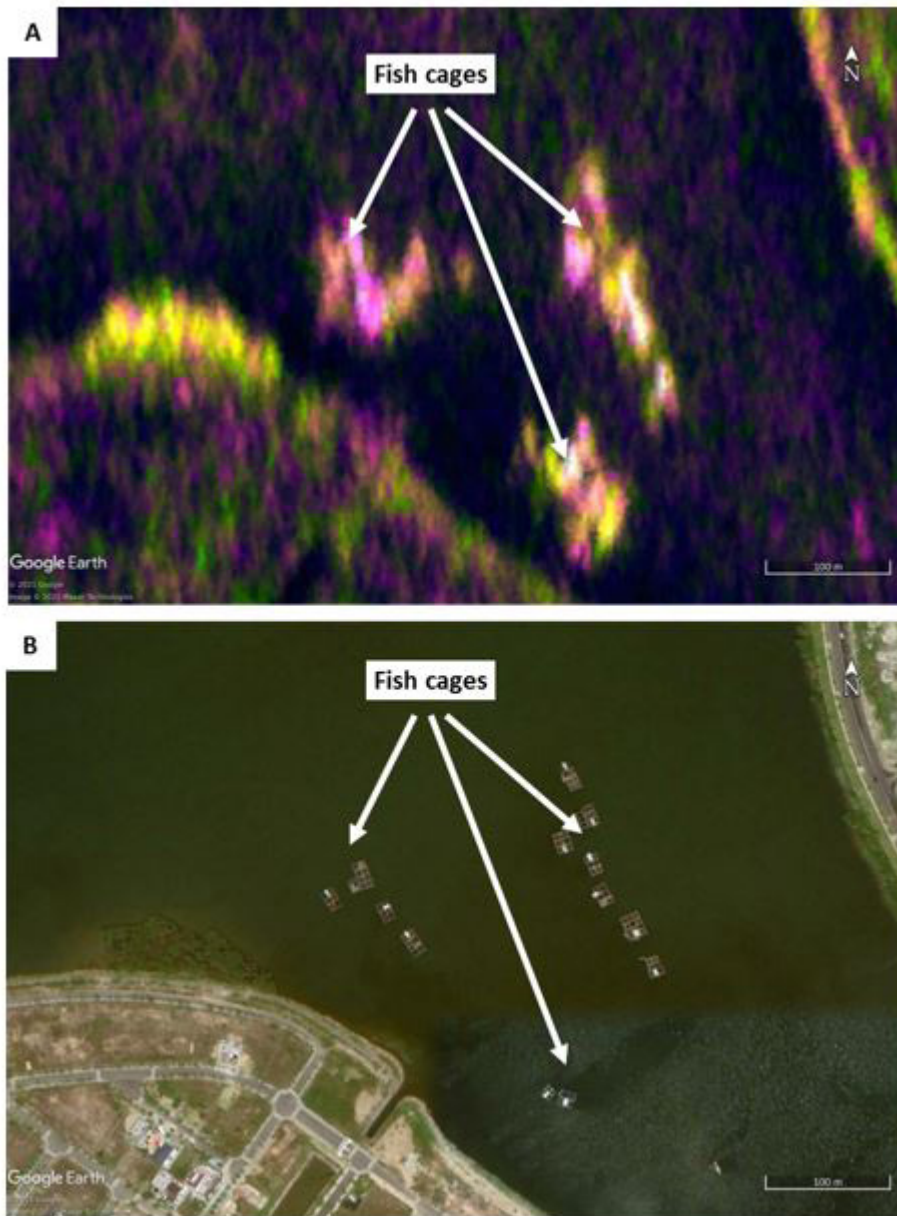


Figure 16: Validation of aquaculture map: A) Sentinel-1 SAR map with aquaculture structures in the middle; B) Google Map high resolution image of the same site.

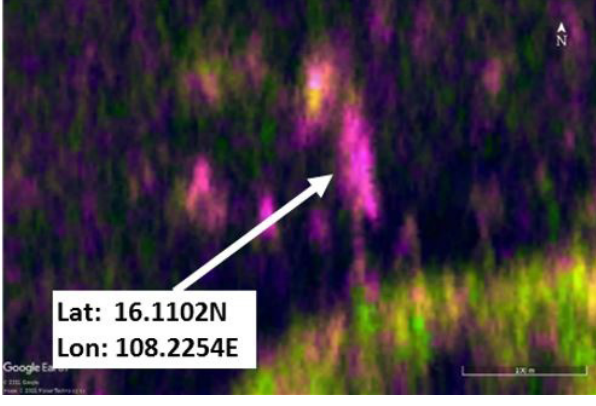

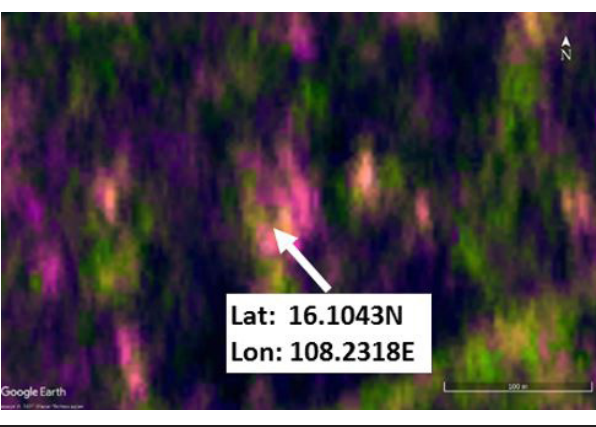

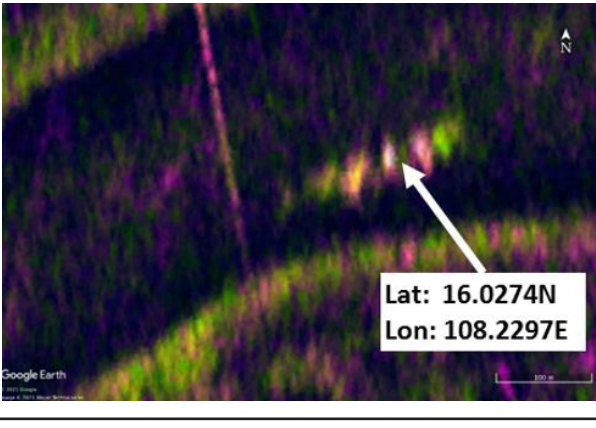
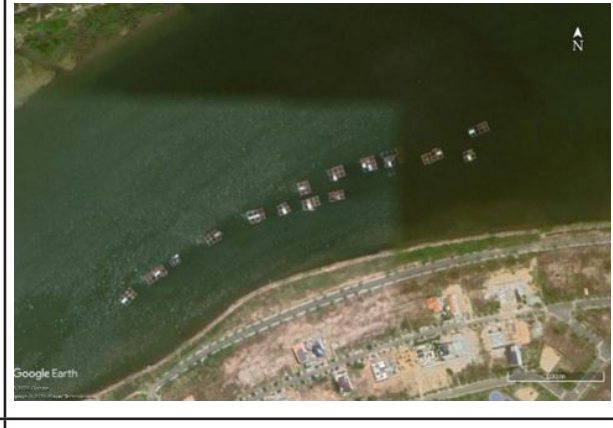
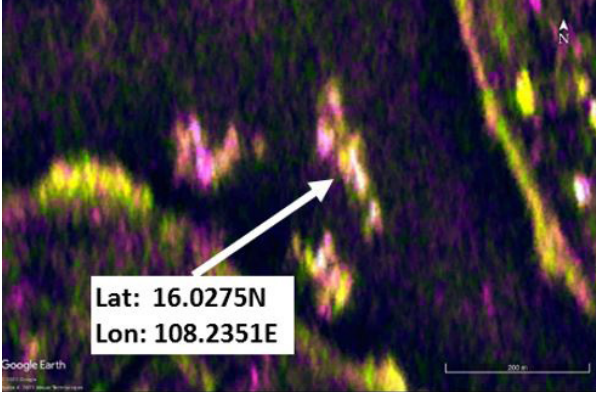

We applied the Google Map satellite images to identify the types of static objects detected in SAR composite maps and to validate the results of detection. Figure 16 shows a close-up view of the potential location of aquaculture site identified earlier in Figure 6. The bright blobs of static objects are clearly seen in the dark background in the middle of SAR image in Figure 16A. The Google Map image in Figure 16B shows rectangular objects of about 15 to 20 meters in size in the same location, identified as floating frames of fish cages. It is worth noting here that Google satellite images are updated on average once a year and they do not match in time with the SAR composite map. For this reason, we expected some inconsistency between Google Maps and SAR satellite data. Nevertheless, very good agreement was demonstrated for the site in Figure 16.

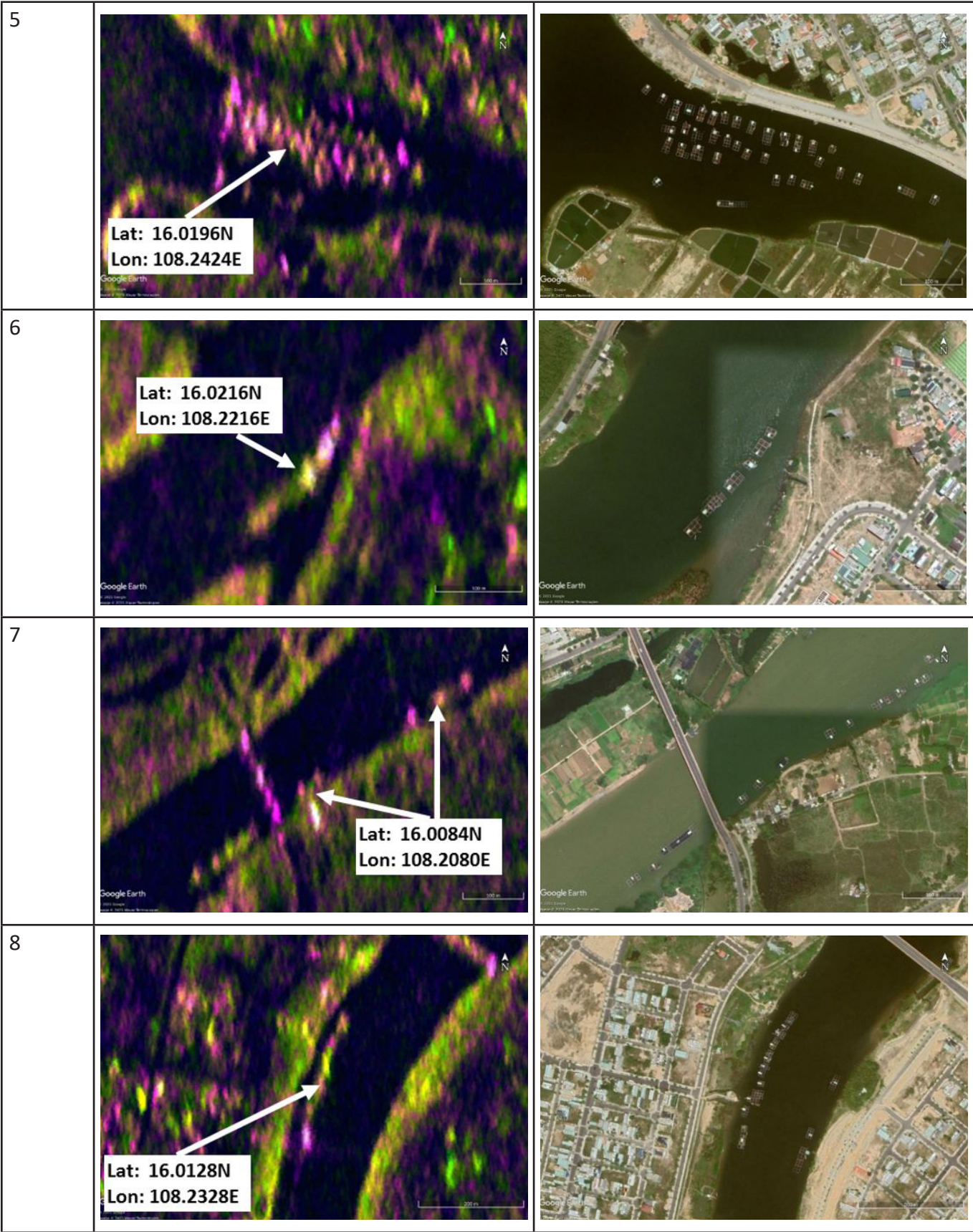


Figure 17: The map of aquaculture sites detected using Sentinel-1A SAR sensor.

To identify aquaculture sites at different locations, the entire SAR composite map of study region in Figure 15 was visually analysed. The positions of candidate aquaculture sites were recorded and then validated using the Google Map Satellite images. For all 11 places identified as potential aquaculture locations in the SAR composite map we found the rectangular objects at Google Maps that resembled fish cages. The positions of detected sites are summarised in the composite map in Figure 17. Four of the sites were found in Da Nang Bay: sites 1 and 2 are located to the West near the entrance of Han River; sites 10 and 11 are located in the opposite direction, at bays Vinh Nam Chon and Vinh Kim Lien. The rest of aquaculture sites are placed along the banks of rivers Song Cam Le and Song Do Toa at the distance of approximately 10 kilometres form Da Nang Bay. The close-up views of all 11 sites in the Sentinel-1A SAR map and high resolution Google Map satellite images are summarised in Table 2. The aquaculture structures are clearly seen in Sentinel-1A SAR data (the second column). The high resolution Google Map images in the third column confirm that the detected objects are aquaculture structures and cages.

**Table 2. A close-up view of the detected aquaculture sites in Sentinel-1A SAR static map and Google Map high resolution images**

| Site No | Senitnel-1A SAR   | Google Map Image   |
|---------|---|--|
| 1       |    |    |
| 2       |   |   |
| 3       |  |  |
| 4       |  |  |



|           |   |  |
|-----------|---|--|
| <p>9</p>  | <p>Lat: 15.9785N<br/>Lon: 108.2208E</p> |  |
| <p>10</p> | <p>Lat: 16.1385N<br/>Lon: 108.1305E</p> |  |
| <p>11</p> | <p>Lat: 16.1623N<br/>Lon: 108.1423E</p> |  |

## 4. Discussion

### 4.1. Earth observations for environmental assessment

Earth Observation (EO) data can provide both a long-term overview of environmental conditions within a region, but also more detailed spatial and temporal resolution to assess local processes and ecosystem health. The datasets used as examples here are now readily available within the ACCORD EO data portal, where they can be easily viewed and investigated using simple plots and analysis online. The datasets can also be downloaded from the data portal for further in depth interrogation.

Here, the lower resolution EO NOAA's Pathfinder SST (4 km) and OC-CCI Chlorophyll a (1 km) datasets were used to demonstrate assessment of larger scale regional climatic patterns. Neither of the regions investigated (Vietnam and Cambodia) showed long-term trends in warming or chlorophyll a concentration, suggesting that climate-scale trends are not yet detectable in these areas using these datasets, which are of about 20 years in length and, thus, longer datasets are required. Further understanding of the contribution of climate indices, such as the El Nino Southern Oscillation, to regional environmental drivers such as temperature is important to consider the long-term changes in conditions. In both regions around Cambodia and Vietnam the highest chlorophyll levels occurred near the coast. However, as discussed in the methods, the OWT and algorithm selection for this dataset are not optimised for coastal and transitional waters, hence, these results need to be interpreted with this in mind.

The high resolution (300 m and 60 m) Calimnos datasets have been used for regional scale observations over varying time-scales (weeks to months). These observations highlight riverine inputs, and local hydrodynamics, local chlorophyll (algae) blooms, and regional temperature regimes (warm and cold currents), which can be used to assess water quality, explain environmental impact events, and when used in conjunction with modelling and in situ observations could assist with synoptic scale monitoring or even forecasting. Indeed, together with the mapping of aquaculture sites, environmental data from these high resolution EO datasets can show areas likely to experience high productivity, and hence be beneficial to aquaculture, or areas with high levels of turbidity or suspended sediment. The 300 m data offer the best balance of resolution and algorithm performance for coastal remote sensing at present, however, as highlighted here, there are some discrepancies between the 300 m and 60 m datasets, especially in the chlorophyll a in some monthly composites. The 60 m dataset is better for highlighting local scale features and very nearshore dynamics.

### 4.2. Earth Observations for mapping location of aquaculture sites

Here we describe and demonstrate a methodology developed for mapping aquaculture structures, such as finfish cages, shellfish farms and floating houses using freely available Sentinel-1A SAR sensor data. It combines a series of satellite images into a map that show the location of static objects on the water surface. This methodology has been successfully applied to detect aquaculture sites in Da Nang Bay and nearby rivers. Two maps of the site were generated in years 2017 and 2019. By using these maps we identified 11 aquaculture sites in the bay and along the rivers. These observations were confirmed by the comparison with high resolution Google Map satellite images that revealed the presence of rectangular aquaculture structures in the same locations. The comparison of static maps in year 2017 and year 2019 demonstrated that in two years the configuration of aquaculture sites has changed in many locations and

new sites were developed. Hence, the proposed methodology can be used not only for the detection of aquaculture sites, but also for monitoring any changes in time. The aquaculture maps based on Sentinel-1A data can be processed on regular basis with updates issued every month or even more frequently, compared to the Google Maps being updated about once per year.

The maps were visually analysed to detect site locations, and this took significant time. The processing time can be reduced by developing automatic approach for static object detection and classification, for example, by using AI and machine learning methods.

## 5. Conclusions

Earth observations can be useful tools for addressing many different objectives, ranging from investigating large scale regional climatic trends in temperature and primary productivity, to small scale detection of both natural features such as river plumes, as well as human activities such as land-use change and aquaculture. This report provides examples of what can be achieved using temperature, chlorophyll and turbidity from three different datasets of varying levels of resolution. These data could be used to advise and support management decisions relating to infrastructure development and land use. All the datasets described in this report are available through the ACCORD EO data portal.

## 6. Acknowledgements

Funding was provided by NERC ODA National Capability.



## 7. References

- Ballester-Berman, J.D., Sanchez-Jerez, P., Marino, A., 2018. Detection of aquaculture structures using Sentinel-1 data. Presented at the EUSAR 2018 - 12th European Conference on Synthetic Aperture Radar, Aachen, Germany.
- Can, N.V., Tuan, P.A., 2012. Marine fish farming in Vietnam.
- Casey, K.S., Evans, R.H., Baringer, W., Kilpatrick, K.A., Podesta, G., Walsh, S., Williams, E., Brandon, T.B., Byrne, D.A., Foti, G., Li, Y., Phillips, S.A., Zhang, D., Zhang, Y., 2011. AVHRR Pathfinder version 5.2 level 3 collated (L3C) global 4km sea surface temperature for 1981-2012.
- Copernicus, 2021a. Copernicus Land Service Lakes Water Quality 300m algorithm theoretical basis document.
- Copernicus, 2021b. Copernicus Land Service Lakes Water Quality 100m algorithm theoretical basis document.
- Crisp, D.J., 2004. The State-Of-The-Art in Ship Detection in Synthetic Aperture Radar Imagery (No. Research Report DSTO-RR-0272). Defence Science and Technology Organisation DSTO Information Sciences Laboratory: Edinburgh, South Australia.
- De Zan, F., Guarnieri, A.M., 2006. TOPSAR: Terrain Observation by Progressive Scans. *IEEE Trans. Geosci. Remote Sens.* 44, 2352–2360. <https://doi.org/10.1109/TGRS.2006.873853>
- Kurekin, A.A., Miller, P.I., Avillanosa, A.L., Sumeldan, J.D.C., 2022. Monitoring of Coastal Aquaculture Sites in the Philippines through Automated Time Series Analysis of Sentinel-1 SAR Images. *Remote Sens.* 14. <https://doi.org/10.3390/rs14122862>
- Lavigne, H., Van der Zande, D., Ruddick, K., Cardoso Dos Santos, J.F., Gohin, F., Brotas, V., Kratzer, S., 2021. Quality-control tests for OC4, OC5 and NIR-red satellite chlorophyll-a algorithms applied to coastal waters. *Remote Sens. Environ.* 255, 112237. <https://doi.org/10.1016/j.rse.2020.112237>
- Ottinger, M., Clauss, K., Huth, J., Eisfelder, C., Leinenkugel, P., Kuenzer, C., 2018. Time series sentinel-1 SAR data for the mapping of aquaculture ponds in coastal Asia, in: *IGARSS 2018 - 2018 IEEE International Geoscience and Remote Sensing Symposium*. Presented at the IGARSS 2018 - 2018 IEEE International Geoscience and Remote Sensing Symposium, IEEE, Valencia, pp. 9371–9374. <https://doi.org/10.1109/IGARSS.2018.8651419>
- Rendon, O.R., Edwards-Jones, A., Kieu, T.K., Marcone, O., Broszeit, S., Beaumont, N., 2022. Characterisation of the inshore marine sectors of Da Nang, Vietnam: A report from the ACCORD project. Plymouth Marine Laboratory. <https://doi.org/10.17031/8XWR-PM23>
- Sathyendranath, S., Brewin, R.J.W., Brockmann, C., Brotas, V., Calton, B., Chuprin, A., Cipollini, P., Couto, A.B., Dingle, J., Doerffer, R., Donlon, C., Dowell, M., Farman, A., Grant, M., Groom, S., Horseman, A., Jackson, T., Krasemann, H., Lavender, S., Martinez-Vicente, V., Mazeran, C., Mélin, F., Moore, T.S., Müller, D., Regner, P., Roy, S., Steele, C.J., Steinmetz, F., Swinton, J., Taberner, M., Thompson, A., Valente, A., Zühlke, M., Brando, V.E., Feng, H., Feldman, G., Franz, B.A., Frouin, R., Gould, R.W., Hooker, S.B., Kahru, M., Kratzer, S., Mitchell, B.G., Muller-Karger, F.E., Sosik, H.M., Voss, K.J., Werdell, J., Platt, T., 2019. An

ocean-colour time series for use in climate studies: The experience of the ocean-colour climate change initiative (OC-CCI). *Sensors* 19, 4285. <https://doi.org/10.3390/s19194285>

Stiller, D., Ottinger, M., Leinenkugel, P., 2019. Spatio-Temporal Patterns of Coastal Aquaculture Derived from Sentinel-1 Time Series Data and the Full Landsat Archive. *Remote Sens.* 11. <https://doi.org/10.3390/rs11141707>

Sun, Z., Luo, J., Yang, J., Yu, Q., Zhang, L., Xue, K., Lu, L., 2020. Nation-Scale Mapping of Coastal Aquaculture Ponds with Sentinel-1 SAR Data Using Google Earth Engine. *Remote Sens.* 12. <https://doi.org/10.3390/rs12183086>

Tuan, L.A., 2003. Status of Aquaculture and associated environmental management issues in Vietnam. Department of International Development, Vietnam.

Ulaby, F.T., Moore, R.K., Fung, A.K., 1982. *Microwave Remote Sensing Active and Passive-Volume II: Radar Remote Sensing and Surface Scattering and Emission Theory.* Artech House: Norwood, MA, USA.

Xuan, T., 2018. Farmers in Da Nang keep raising fish in river despite ban. *Tuoi Tre News.*

